ANALYSIS OF AN ON-OFF
MODULATED CLUTCH SERVO-MECHANISM

WILLIAM B. DUNCAN
and
WILLIAM V. SURMAN, JR.

ANALYSIS OF AN ON-OFF MODULATED
CLUTCH SERVOMECHANISM

* * * * *

William B. Duncan

and

William V. Surman, Jr.

ANALYSIS OF AN ON-OFF MODULATED

CLUTCH SERVOMECHANISM

by

William B. Duncan

Captain, United States Marine Corps

and

William V. Surman, Jr.

Lieutenant, United States Navy

Submitted in partial fulfillment of
the requirements for the degree of

MASTER OF SCIENCE

IN

ELECTRICAL ENGINEERING

United States Naval Postgraduate School
Monterey, California

1960

ANALYSIS OF AN ON-OFF MODULATED

CLUTCH SERVOMECHANISM

by

William B. Duncan

and

William V. Surman, Jr.

This work is accepted as fulfilling

the thesis requirements for the degree of

MASTER OF SCIENCE

IN

ELECTRICAL ENGINEERING

from the

United States Naval Postgraduate School

ABSTRACT

This thesis presents an analysis of a nonlinear servo-mechanism. The nonlinear control device is an electro-mechanical spring clutch designed by the Propeller Division of the Curtiss-Wright Corporation for use in both missiles and manned aircraft.

A mathematical representation of the system is first derived. Then an analytic technique is presented which may be employed to predict such closed-loop response characteristics as gain, phase shift, and bandwidth.

Investigations are made regarding both the absolute stability and the relative stability of the system, however, only limited conclusions are reached due to the lack of established stability criteria for a system of this type. Recommendations are made for further study of the stability of this system for the purpose of establishing such criteria.

The ground work for this thesis, including the preliminary analysis and all of the equipment tests, was accomplished by the authors during the summer of 1960 while on an industrial experience tour at the Missiles and Space Division of the Lockheed Aircraft Corporation, Sunnyvale, California. The authors are extremely grateful for having had the opportunity to do this work at Lockheed Missiles and Space Division. Particularly, appreciation is expressed to Mr. Fred A. Schupan of Lockheed, for his very able guidance and assistance through-

out the conduct of the analysis. Appreciation is also expressed to Messrs. Richard Lawhorn, Kenneth Alder, and Charles Cox, of Lockheed, for their assistance on various aspects of this work.

The authors gratefully acknowledge the advice and assistance given by Professor Robert D. Strum of the United States Naval Postgraduate School during the writing of this paper.

TABLE OF CONTENTS

LIST OF ILLUSTRATIONS

LIST OF ILLUSTRATIONS

LIST OF ILLUSTRATIONS

vii

CHAPTER I

INTRODUCTION

General

In the field of control engineering a search is
continually being made for new and improved methods
for optimizing system response. The missile industry
in particular has presented the control engineer with a
challenge which will tax his ingenuity to the utmost if
he is to supply the control devices to meet the exacting
demands of the field.

Various methods of control are presently in use
throughout industry, the most common of which are a-c
servomotors, d-c control motors, hydraulic controls,
pneumatic controls, contactors or relays, and clutches
and brakes. Any one of these methods may very well offer
definite advantages over all the others in a particular
application. Many of these devices have found wide appli-
cation because they are linear in nature and thus are well
suited to straightforward linear mathematical analysis.
On the other hand, the development of other of these de-
vices which are nonlinear in nature has been considerably
slower because of the complexity of nonlinear mathematical
analysis. It is pointed out, however, that due to the ex-
tremely rapid growth of the control engineering field, and
the common prevalence of nonlinearities in control systems,

1

the nonlinear problem has received a great deal of attention in recent years, and it is no longer the nemesis to the development of nonlinear control devices that it was a decade ago.

Purpose of Paper

It is the purpose of this paper to present an analysis of a nonlinear servomechanism. This nonlinear control device is an electromechanical spring clutch designed by the Propeller Division of the Curtiss-Wright Corporation. As early as 1952 a general study was made by Stuelpnagel and Dallas [1] emphasizing the advantages of a system employing basically the same principles that are incorporated in this system. The electromechanical spring clutch is, however, entirely new in design and construction, and its improved characteristics will serve to further advance the state of the art for clutch type servomechanisms.

Scope of Study

This paper presents an analysis of the electromechanical spring clutch functioning as the control element in a single-loop unity feedback system. A combination of techniques are employed in the conduct of the analysis. The analytic technique is used quite extensively since it is this approach which leads most naturally to suggestions for means to improve system performance through the use of compensation. More specifically, two mathematical approaches

2

are utilized. Both make use of Kochenburger's [2] describing function. First, a method devised by Levinson [3] is used to determine the closed-loop response of the system to a range of inputs. The Levinson technique yields system output magnitude and phase versus frequency. The system bandwidth, being a characteristic of primary interest in any servo system, is readily discernible from a plot of this information. The other analytic approach employed is one wherein the describing function and the linear transfer function are plotted on a Nyquist diagram. From this plot limit cycle data and other system stability information may be obtained.

A second technique which may be very useful in any analysis is the trial and error approach on the analog simulation of the system. The analog computer is most useful in the absence of the actual equipment itself. Since the actual clutch was available for this study, the analog technique found only limited use.

The final technique employed in this analysis is the conduct of a series of tests on the system itself. These equipment tests, in addition to spelling out exactly what the system can do performance-wise, serve as a check on the validity of the mathematical representation used in this analysis.

Some Advantages of Clutch-type Servomechanisms

Clutches are widely used in control systems that range in size up to thousands of horsepower. Clutch-type servo

actuators compete with a-c servomotors in sizes up to one horsepower and with d-c servomotors over the whole power spectrum. One of the most important considerations in servomechanism design is the speed of response. High speed response is difficult to obtain with a typical servomotor control device because of the inertia of the motor armature. However, when using a servo clutch driven by a continuously running motor, such as the one under discussion in this paper, the inertia of the motor armature tends to improve system response time, rather than hinder it. The servo clutch actually utilizes the energy stored in the armature of the continuously running motor to give the system a high starting acceleration. Comparative acceleration characteristics of a typical servo clutch, and typical servo motor are shown in Figure 1. It is seen that the servo clutch accelerates at 30,000 radians per second per second or five times faster than the typical servo motor. Though not shown in this figure it is pointed out that the electromechanical spring clutch accelerates at 130,000 radians per second per second, or more than 20 times as fast as the servo motor.

The electromechanical spring clutch, like most other servo clutches is actuated by an electromagnet. With this in mind, another major advantage of the servo clutch is pointed out. The magnetic clutch is a very effective transducer of power from electrical to mechanical form. It transforms and amplifies power in the same operation. A comparison
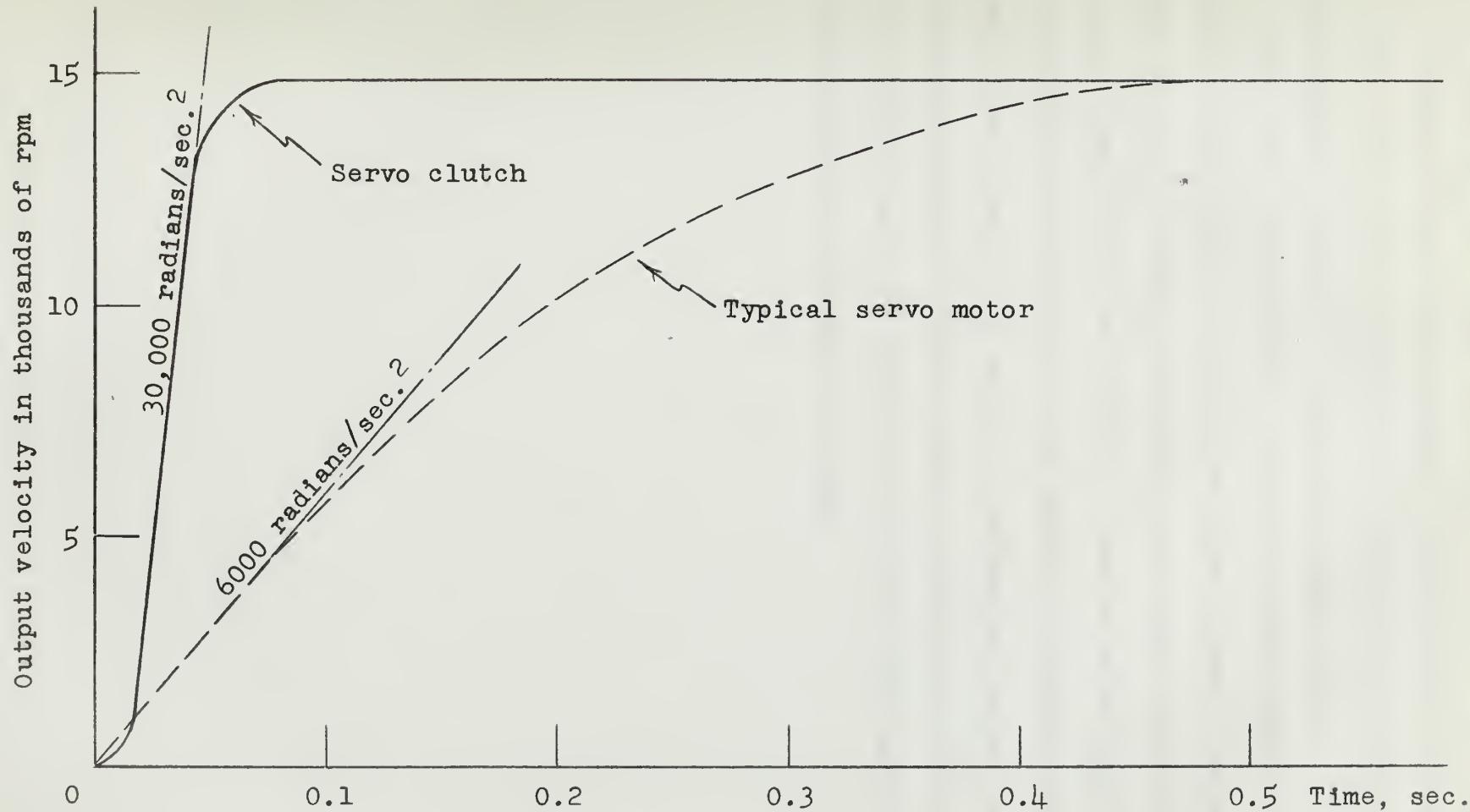
Figure 1.   Comparative acceleration characteristics of a typical
servo clutch and typical servo motor

is made between a typical 300-watt output servo motor and a 300-watt output servo clutch. In the case of the servo clutch, 300 watts of mechanical output power may be controlled by 10 watts of electrical input power. A 300-watt output from a servo motor, however, would require approximately 500 watts of controlled input power. In this comparison it is readily seen that the servo clutch alone shows a power amplification of 30 to 1 and an advantage over the servo motor of 50 to 1 in the amount of electric power required to control 300 watts of mechanical output power. The electromechanical spring clutch is even more effective, for it requires but 2.24 watts of electric input power to control a 456-watt mechanical output.

CHAPTER 2

DESCRIPTION OF EQUIPMENT

General

Before giving a detailed description of each of the
system components, a few remarks will be made regarding
the system as a whole. The system is an on-off modulated
type of servomechanism. The block diagram of Figure 2
shows the relationship of the various components.

The signal source might be, for example, from the gui-
dance package of a missile. The output of the servo ampli-
fier energizes (depending upon its polarity) one of the two
electromagnets within the clutch. One magnet causes the
clutch to drive in one direction whereas the other causes
it to drive in the opposite direction. Servo power is ob-
tained from the continuously running drive motor. The drive
motor output speed is 4230 revolutions per minute. The cor-
responding clutch output speed is 2500 revolutions per min-
ute. The linear actuator converts the rotary output motion
of the clutch to a linear motion. Additional gearing is
then used for angular positioning of the load, a maximum of
plus or minus 25 degrees from a central position.

Photographs illustrate the actual equipment test set-up
utilized for the analysis. See Figures 3 and 4.

7

8
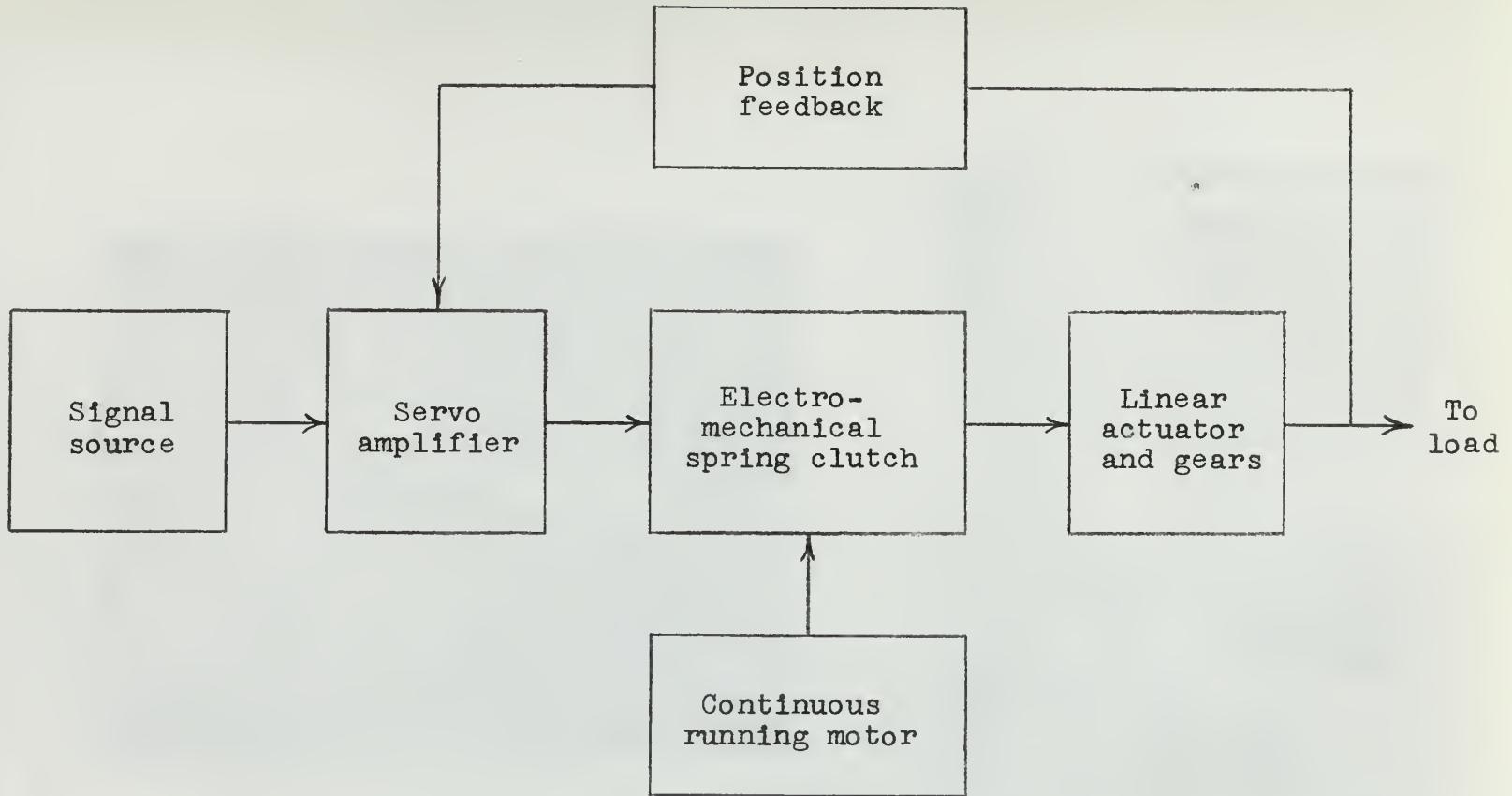
Figure 2. Block diagram of on-off modulated clutch servomechanism
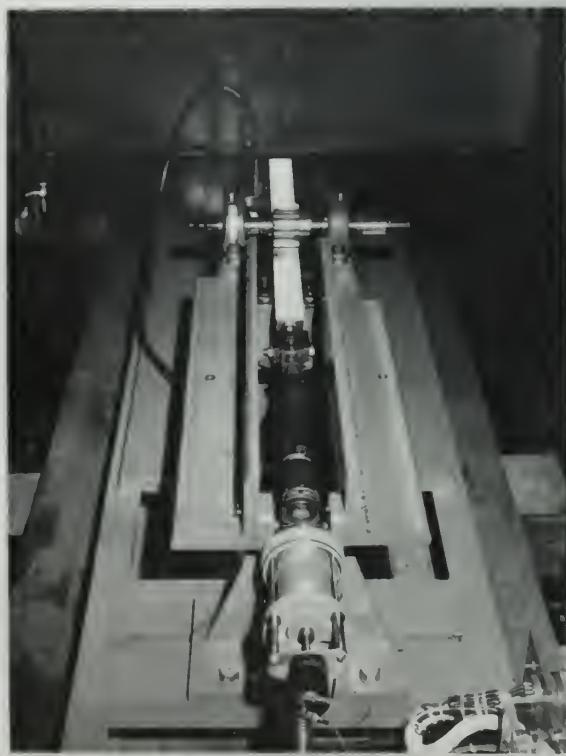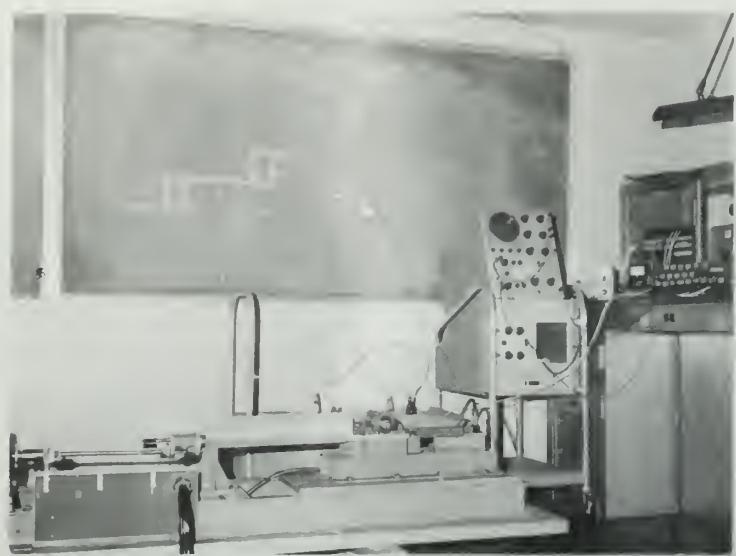
Figure 3. Laboratory set-up of closed loop system

9
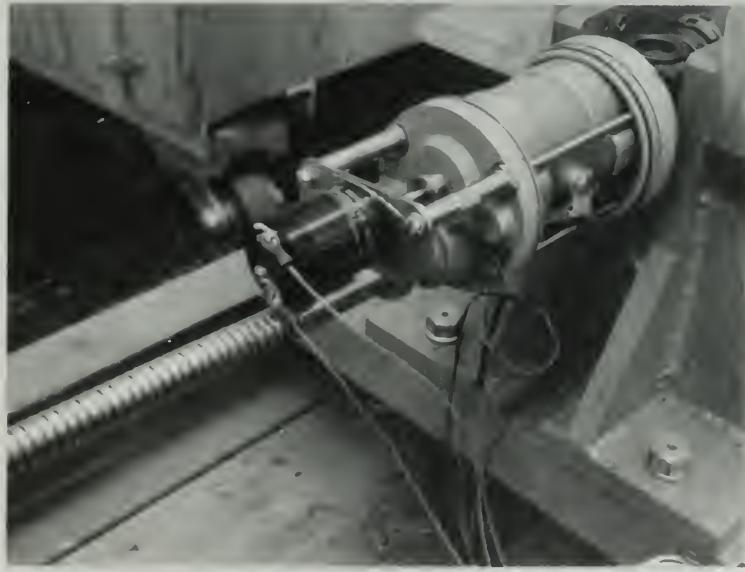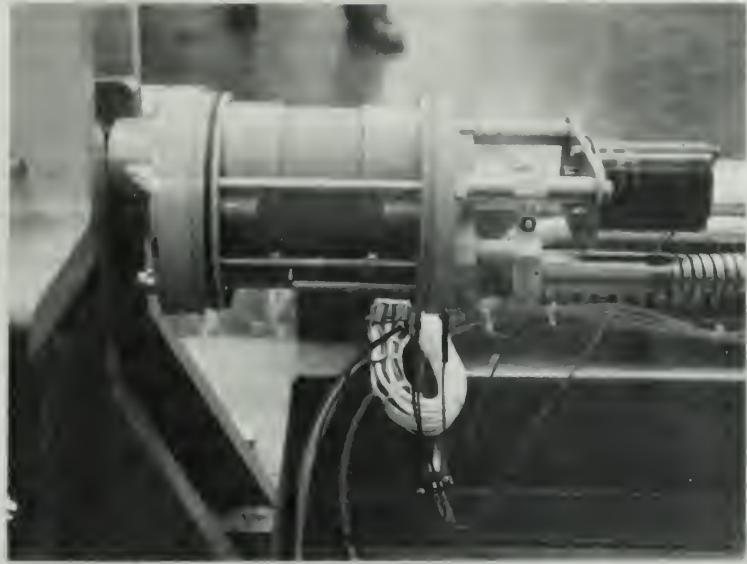
Figure 4.   Close-up of clutch with tachometer as used
            in laboratory tests

10

Electromechanical Spring Clutch

The physical size and weight of this clutch mechanism are important advantages, for the clutch is but 5.1 inches long and weighs only 4.9 pounds.

An understanding of the electromechanical spring clutch is facilitated by familiarization with the nomenclature of the clutch assembly and examination of the sequence of events of operation. See Figures 5 and 6.

The electromechanical spring clutch consists of the following parts:

Clutch housing	1	Clutch disk	2
Rotary input drive	1	Clutch spring	2
Fixed shaft	2	Rotary output drum	1
Rotor	2	Flexible shaft output	1
Electromagnet	2	Interlock mechanism	1

Examination of the electromechanical spring clutch is simplified by realizing that operation clockwise or counterclockwise is identical and it is adequate to examine the sequence of events for a given direction of rotation. Use of Figure 5 and an artist's cut-away sectional drawing, Figure 6, greatly facilitate tracing the sequence of events.

Mechanical input to the clutch mechanism is a constant speed of 4230 revolutions per minute through gearing to the rotors, imparting a 2500 revolution per minute constant speed to the output drum when the clutch is completely engaged and

11
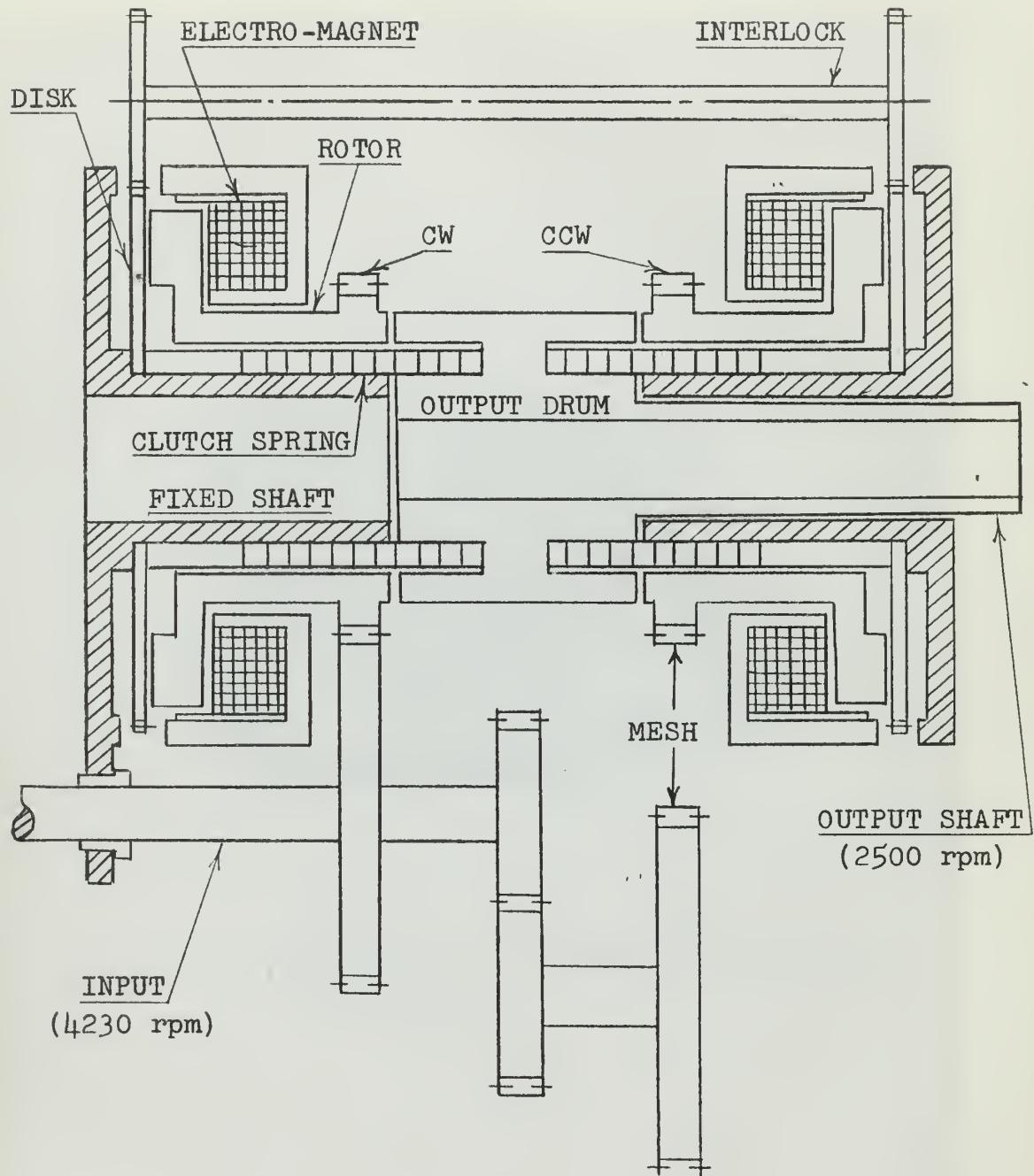
Figure 5. Functional schematic of clutch

12
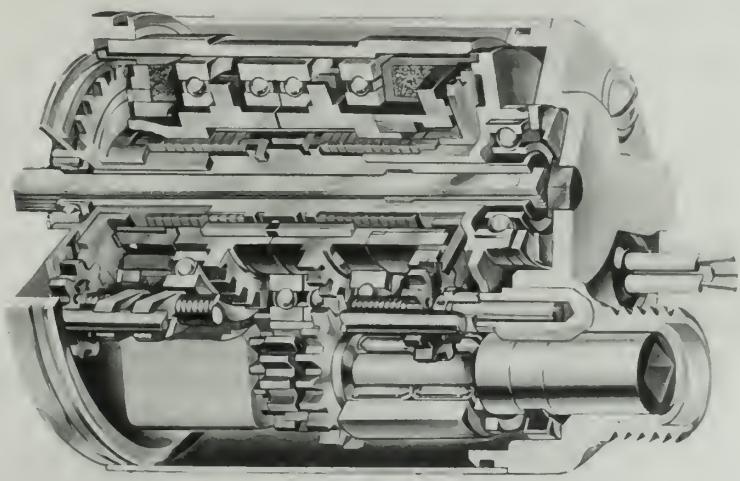
Figure 6.   Cutaway view of electro-mechanical
spring clutch

transients no longer exist.

The electrical input to the clutch from the servo amplifier energizes the coil of an electromagnet. The magnetic force attracts its associated clutch disk with sufficient force to hold it against the constant speed rotor. Friction between the clutch disk and rotor surface draws the clutch disk around with the rotor. The associated clutch spring is then unwrapped by the clutch disk engaging a lug at the disk end of the clutch spring. As the clutch spring is unwrapped its outer surface grabs the inner sleeve-like surfaces of the driving rotor and the output drum. The clutch spring is maintained open with a comparatively light force by the clutch disk on the end of the spring. A sufficient torque to drive the output drum is transmitted from the driving rotor through the clutch spring. A flexible laminated spring shaft rigidly attached to the output drum then drives the output mechanism in a rotary fashion.

The clutch is directed to stop by removing the electrical input to the servo amplifier which de-energizes the coil of the electromagnet. The clutch disk then slows, causing the force to be removed from the lug on the end of the clutch spring with a resultant relaxation of the clutch spring. This relaxation of the clutch spring on its respective fixed shaft causes a braking action to be imparted through the clutch spring, which is rigidly attached to the output drum, and hence to the load.

14

The interlock gear and shaft mechanism prevents both ends of the clutch from engaging their respective clutch disks and clutch springs at the same instant and maintains the non-driving spring in a relaxed position.

Linear Actuator, Gears, and Load

The rotary output of the clutch is converted to a linear output through a ball-screw type actuator. The linear output rate of this actuator is 5.42 inches per second at the rated input of 2500 revolutions per minute to the actuator. It is interesting to note the efficiency of this ball-screw type actuator is 90 percent[1] compared to approximately 53 percent for a comparable rotary type actuator.

The linear output then couples directly to a rack and pinion type gear arrangement to which may be attached rotary inertia loads and friction drums. See Figure 3.

A linear potentiometer with the pick-off tap fixed to the linearly driven rack gear is utilized to supply position feedback to the servo amplifier.

Servo Amplifier

Figure 7 is a block diagram showing the important features of the amplifier which is used to control the electrical input to the clutch.

―――――――――――

[1]Efficiency values are quoted from manufacturer's specifications.
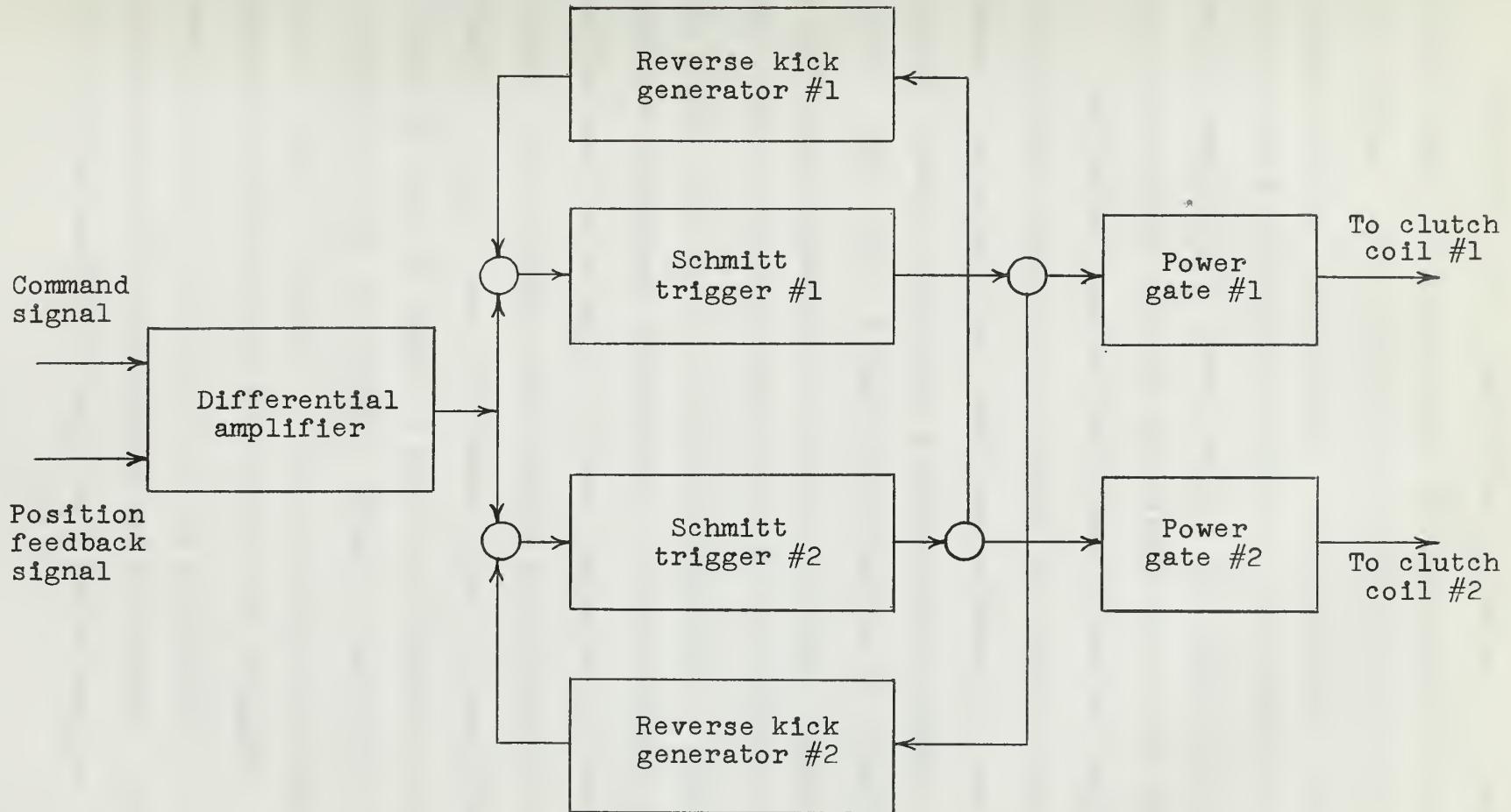
Figure 7. Block diagram of servo amplifier used with the electro-mechanical spring clutch

16

The differential amplifier produces a voltage at its output which is proportional to the voltage difference of the two inputs. It is designed to operate about a d-c voltage output level of seven volts. In other words, when the two inputs add algebraically to zero, the output of the differential amplifier is seven volts. The amplifier gain may be adjusted without varying the bias level of the output.

Preliminary system tests were conducted using only the differential amplifier to excite the clutch coils. For these tests, the output bias level was adjusted to zero. This resulted in merely applying a proportional signal to the clutch coils. This type of input was found to be unsatisfactory. At a particular magnitude of the proportional signal, the clutch was found to be at a point where it was about to engage, but the signal was not of sufficient strength to cause full or positive engagement immediately. This resulted in slippage within the clutch which in turn caused excessive heating of the clutch. To overcome this problem an electronic relay, the Schmitt trigger, was introduced into the amplifier circuit. As can be seen in Figure 7 two such triggers are used. The operation of the two Schmitt triggers can best be understood by referring to Figure 8. It is readily seen that there is present in the firing cycle of the two triggers a slight hysteresis effect. As long as it is kept small it will not seriously affect the performance of the system. Hysteresis will be discussed more fully in a later section. The object

17
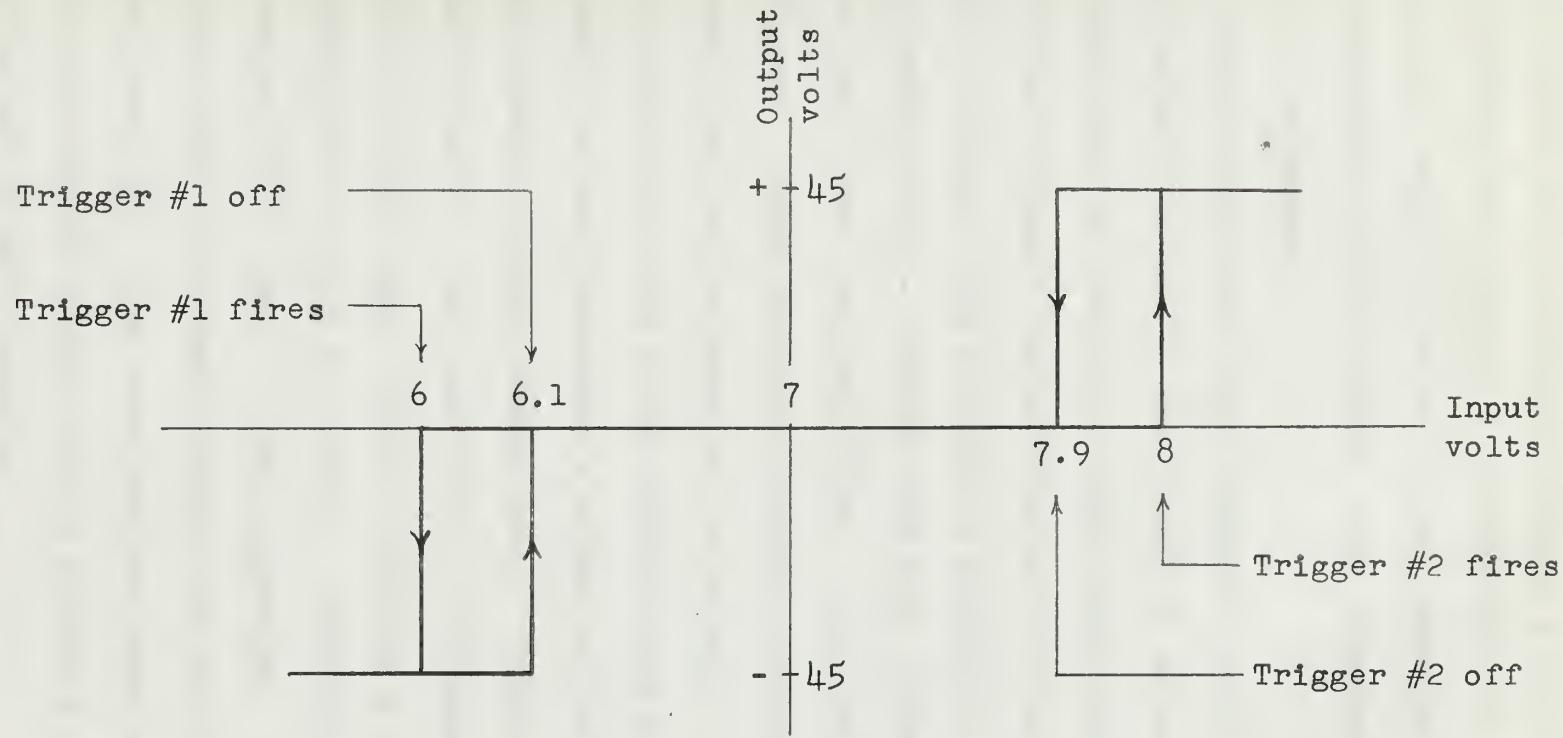
Figure 8. Schmitt trigger firing cycle

of using the Schmitt trigger, then, is to delay the signal to the clutch coils until it reaches a threshold value, and upon reaching this value, a voltage will be applied to the clutch coils which is of sufficient strength to insure positive engagement of the clutch, thus eliminating any possibility of slippage.

Initial open-loop tests conducted on the system indicated the delay in stopping the clutch to be considerably longer than the delay in starting. Since these delays have great effect on the response characteristics of the system it was desirable to reduce them as much as possible, particularly the long stopping delay. Toward this end, a reverse kick generator was built into the amplifier. Its operation is explained as follows. Assume that coil number one has been energized for some time, and is about to be cut-off. When trigger number one cuts off, this fires reverse kick generator number two, which in turn generates a signal of sufficient magnitude to fire Schmitt trigger number two. Clutch coil number two is thus energized, the associated electromagnet clamping the number two clutch disk, thereby creating a drag which assists in bringing the clutch to a stop. Obviously the duration of the reverse-kick signal is very important. If it is too long the clutch will not remain stopped but will drive in the opposite direction. Thus provision was made so that the duration of the reverse-kick signal may be adjusted to any length between two and 25 milliseconds.

The power gates serve merely to supply the clutch coils with a signal of desired magnitude, once the Schmitt triggers have fired.

CHAPTER III
PERFORMANCE CRITERIA FOR THE SYSTEM

Performance specifications in servo literature follow no universal pattern and are as numerous as there are authors. Even the more completely developed linear servo field lacks uniformity, therefore, prior to listing the specifications it seems appropriate to discuss some of the major items which must be considered in the establishment of criteria for a system of this type.

Since there is an exact correspondence between the operation of an on-off clutch control circuit and the circuits of on-off relay control, [4], the criteria to be discussed below are precisely that prescribed in the literature, [5], for contactors and relays.

In an on-off control system one of the major design considerations is static accuracy. By this it is meant, the range of error which can exist when the servo is in a state of rest without initiating corrective action. This requirement is met by keeping the range of the inactive zone within specified limits. The narrower the inactive zone, the greater will be the static accuracy of the system. However, narrowing the inactive zone tends to increase system gain and thereby decrease system stability. Thus it is seen that a compromise between static accuracy and stability considerations may be necessary.

A second consideration is that of dynamic accuracy, or the extent to which errors are minimized when the system is responding to a disturbance. The accuracy of a system under dynamic conditions is dependent upon the speed of response and the degree of stability. The speed of response is in turn, dependent upon the runaway correction magnitude. (The runaway correction magnitude, R , is defined as the steady-state rate of change of the output that would be approached if the clutch were to remain engaged for a sufficiently long period.) The higher this magnitude, the faster the system responds to a given disturbance. But, as in the case of decreasing the inactive zone, increasing the runaway correction magnitude corresponds to an increase in gain and therefore generally tends to make the system less stable. Here again, a compromise is necessary between speed of response and stability considerations.

Another major consideration with regard to establishing performance specifications is that of system stability. What is the absolute stability of the system, and what is the degree of stability? As to the absolute stability, an on-off control system may come under one of the following categories:

1) Be completely stable. Here there is no tendency for self-sustained oscillations or for constantly increasing errors following a disturbance.

2) Have self-sustained oscillations of a definite amplitude following the application of a sufficiently large disturbance.

22

3) Be conditionally stable. In this case, either the
system has no output oscillations, or such oscillations are
limited to a given amplitude provided the disturbances to
it do not exceed some critical value. Disturbances above
this value can cause unstable operation to result.

4) Be unstable. In this case, any disturbance, no
matter how small, results either in a constantly increasing
error or in oscillations which increase in amplitude toward
destructive breakdown.

Now, the degree of stability takes on a different mean-
ing depending upon the category of absolute stability. For
systems which are always stable, "degree of stability" refers
to the rate at which the oscillations resulting from a given
disturbance are damped. This is not to be confused with the
"damping ratio" of linear systems. In the on-off control
system the pattern of such damped oscillations is dependent
upon the magnitude of the disturbance, and constants such as
"damping ratio" and "logrithmic decrement" have no signifi-
cance.

For systems which maintain self-sustained oscillations,
"degree of stability" takes on a slightly different meaning.
Suppose a large disturbance is applied to a system of this
type. The initial oscillations may be of large amplitude,
but these oscillations diminish in amplitude until the steady-
state amplitude of the sustained-oscillation condition is
reached. Specifications can be established in terms of the

time required for oscillations to be reduced to a specified amplitude following a given disturbance.

Conditionally stable systems might be acceptable where it can be assured that no disturbance will ever occur of such a magnitude as to cause instability. In such a case, degree of stability specifications may be applied similar to those outlined above.

Still another factor which warrants some consideration and may be prescribed in the performance specifications is the number of engagements the clutch makes. The reason for this is obvious. The greater the number of engagements, the greater the wear on the clutch and the greater will be the heat generation within the clutch.

As mentioned previously the size of the inactive zone plays an important part in determining static accuracy, dynamic accuracy, and stability in general. It is also extremely important in regard to number of clutch reversals required to bring the clutch to a stop with zero error. The clutch must be stopped before it crosses the dead zone, or it will drive full speed in the opposite direction and will never be brought to a stop. Thus it is evident that both the inactive zone and runaway correction magnitude must be studied jointly in an effort to solve the stopping problem.

In summary, let it be said the above discussion by no means covers all the details that must be considered in establishing the performance criteria for an on-off type servo.

It is only meant to emphasize some of the major considerations involved in such a process. It may be said then, that the performance requirements for the on-off system may be met by specifying a range of inactive zone consistent with static accuracy requirements and a runaway velocity consistent with the desired speed of response. These, of course, must be chosen with an eye toward adequate stability which may or may not require some compensation effort.

Having in mind the factors which must be considered in arriving at a set of specifications the following performance criteria[1] are listed:

Runaway correction magnitude, $R = 175°/sec$
Width of the inactive zone, $\Delta = 1°$ to $2°$ (range)

These specifications define an adequate servo system and are kept quite general remembering that the purpose of this paper is to present an analysis of this system. Other characteristics of the system operating under these specifications are to be determined from the analysis. Detailed compensation and optimization are not objectives of this investigation and will be mentioned only briefly in ensuing sections.

---

[1]Design characteristics of the equipment test set-up, inactive zone, and runaway correction magnitude were established by Lockheed Aircraft Corporation as typical requirements suitable for flight control application.

CHAPTER IV

PRELIMINARY ANALYSIS

General

A series of preliminary tests were conducted on the
open-loop system in an effort to determine accurately any
time delay characteristics the clutch might possess, and
to establish one other very important point, the effect of
load on the response characteristics of the clutch. The
effect of load would have considerable bearing on the scope
of the closed-loop analysis. Refer to Figure 9 for a
diagram of the system on which these preliminary tests were
made. The tests were conducted for various conditions of
externally applied load at various magnitudes of command
signal. Three magnitudes of a step function input were
used; 28, 45, and 60 volts, as measured at the coils of the
clutch. The load conditions were 0, 20, and 45 ft-lbs of
torque applied externally by means of a friction drum. In
addition to this applied torque, an inertia disk was added
at the output, resulting in another 6.2 slugs mass at the
output of the actuator.

Delay Characteristics

Table I is a summary of the results obtained in the
preliminary tests. Figure 10 shows oscillogram traces of
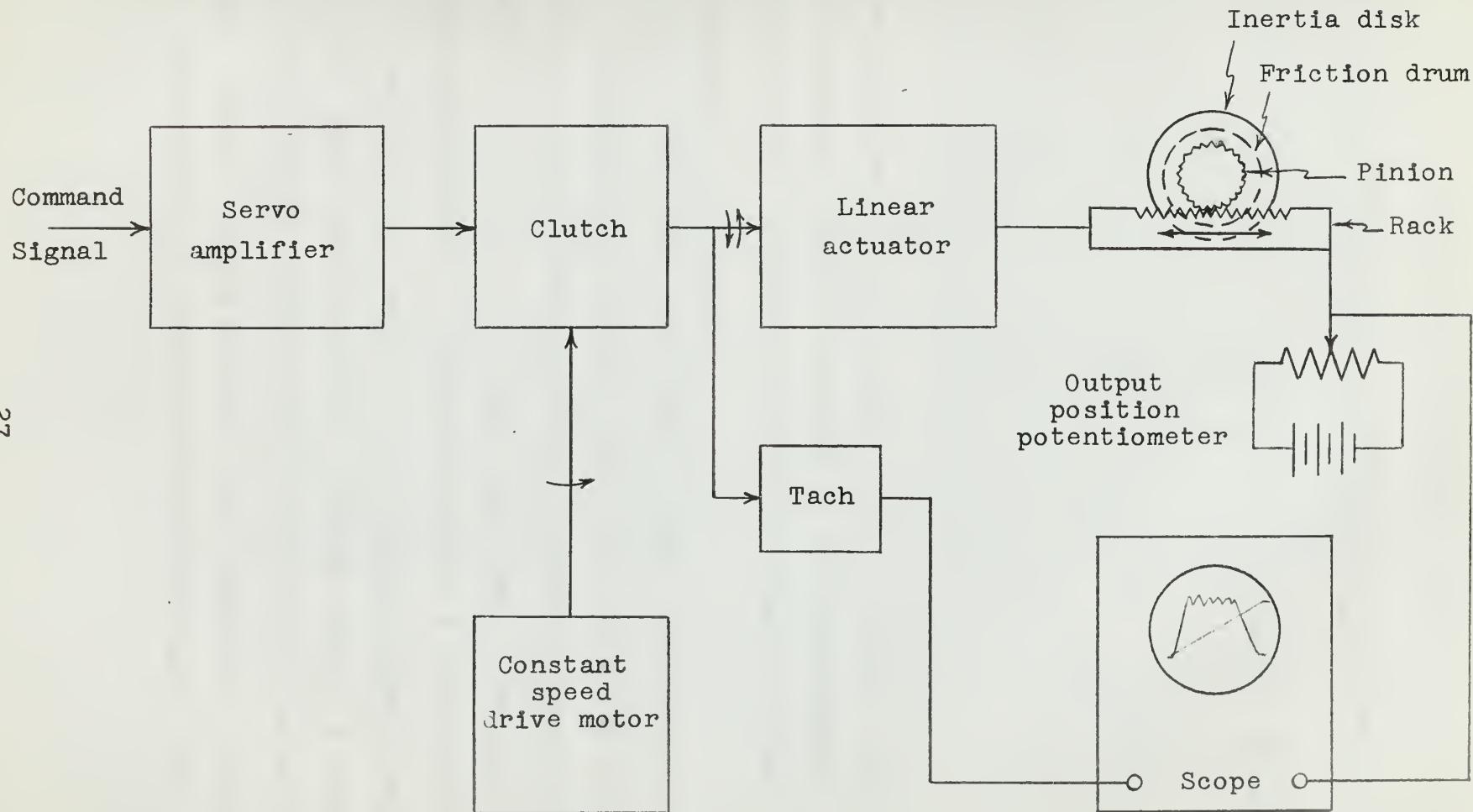
Figure 9. Block diagram of system for preliminary analysis

27

Table I

Results of Preliminary Tests

	Coil Voltage	Load Condition	Delay Start	Stop
(1)	28 volts	0 ft-lb	12 msec	45 msec
	"	20	"	"
	"	45	"	"
(2)	45	0	8	45
	"	20	"	"
	"	45	"	"
(3)	60	0	8	45
	"	20	"	"
	"	45	"	"

the position and velocity outputs for (2) above. Figure 10(a) shows the delay time for starting to be approximately 8 msec, and Figure 10(b) verifies the stopping time to be that given in condition (2) of Table I.

These tests were made using a simple variable gain amplifier. Observing the stopping time to be undesirably long, the amplifier circuitry was modified to include the reverse kick generator in an effort to reduce this time. See Figure 7. Through experimentation it was found that a reverse kick of about 5 msec duration would give a stopping time of approximately the same duration as the starting delay. A reverse kick of any longer duration would cause full reversal of the clutch. Then, by using a reverse kick applied to the opposite coil, the starting and stopping delays were made equal. This

28

0 ft-lb

20 ft-lb

45 ft-lb

msec 40   20   0
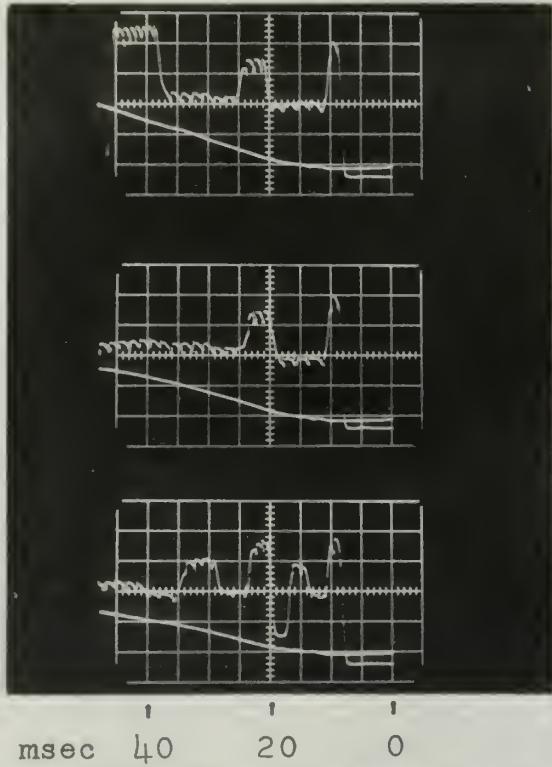
(a)   Starting characteristics

msec 80   40   0
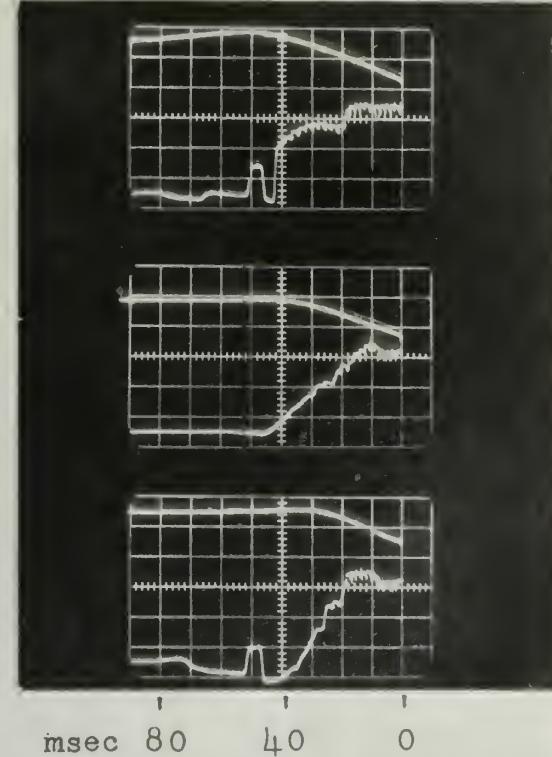
(b)   Stopping characteristics without kick-back

Figure 10.   Delay characteristics of clutch under various conditions of load and 45 volts to coil

29

will, of course, simplify the mathematical analysis of the closed-loop system.

A limit cycle analysis indicated that seven milliseconds was a more representative value for the magnitude of the delay of the system, thus it was believed that the magnitude of the delay was reasonably well established. In the mathematical analysis to follow, the delay will be represented as a transportation lag, ϵ^{-st}, where t = 7 msec.

Effects of Load

The manufacturer's specifications indicate that the clutch is designed to respond to load torques of 25.1 in-lbs at the clutch output shaft without slippage. This corresponds to a load torque of 180 ft-lbs at the output of the system under analysis. Though the clutch is capable of responding to loads of such magnitude, the range of interest in this analysis extends only to approximately 50 ft-lbs thus loads beyond this magnitude were not applied in the preliminary tests. Now the effect of load on the response characteristics of the clutch was determined from actual tests to be negligible. These results were as follows:

Load Condition	Acceleration Time
0 ft-lb	1.0 msec
20	1.0
45	1.0

These data may be read directly from the velocity curves of

Figure 10(a). Similarly no appreciable effect is observed in the stopping characteristics shown in Figure 10(b).

These results indicate that for loads within the range of interest, the response time of the clutch is not affected by load. With this information in mind, it was concluded that no further investigations into the effects of load on response time need be made.

CHAPTER V

MATHEMATICAL REPRESENTATION OF CHARACTERISTICS

Clutch Characteristics

It was learned in the preliminary analysis that the clutch operates essentially as an on-off control device with a constant time delay. That is to say, the clutch, in responding to a disturbance, remains at a standstill during the delay, after which time it is driving at full speed. It was established that the acceleration time in attaining full speed from a standstill is approximately 1.0 msec. This time is negligible when compared with the delay, for example. Thus, for analysis the clutch will be considered a nonlinear on-off device possessing hysteresis.

Mathematically then, the clutch will be represented by both a transfer function, G_s , and a describing function, G_d . The transfer function will actually represent the dynamics of the clutch and actuator. The describing function will serve as a mathematical representation of the on-off characteristics of the system. The delay previously established will take the form of a transportation lag, ϵ^{-st}, in the mathematical representation of the system. Figure 11 shows, in block diagram form, the system arrived at for the mathematical analysis. It will be noted that no amplifier is shown in this diagram. The amplifier gain is, of course, taken into account in the magnitude of the inactive zone of the nonlinearity. A decrease in
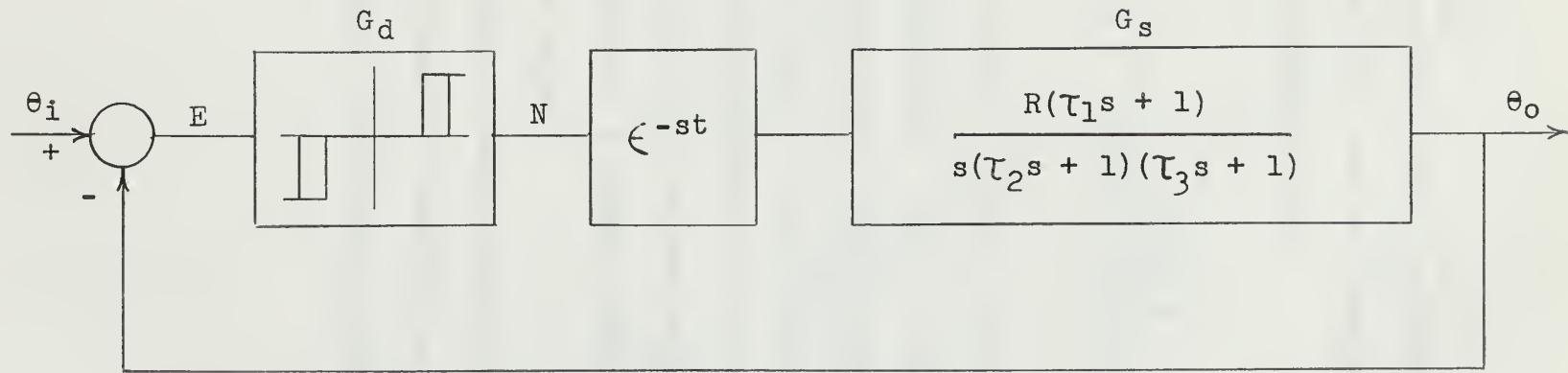
Figure 11. Mathematical representation of system

the size of the inactive zone corresponds to an increase in amplifier gain.

Transfer Function, G_s

The transfer function which represents the linear components of the system will now be developed. As shown in Figure 11 it has the general form

$$G_s = \frac{R(\tau_1 s + 1)}{s(\tau_2 s + 1)(\tau_3 s + 1)} ,$$

where $R = 175^\circ/\text{sec}$ is the runaway correction magnitude set forth in the specifications. The τ terms, which will be derived below, represent the clutch dynamics as well as those of the actuator and the rack and pinion. The linear factor s, in the denominator of the transfer function, represents a single order pole at the origin of the complex s-plane and it identifies a system having a sustained rate for a constant input signal.

To give the reader a better understanding of what is represented by the transfer function, a block diagram showing the mechanical features involved is presented in Figure 12.

34
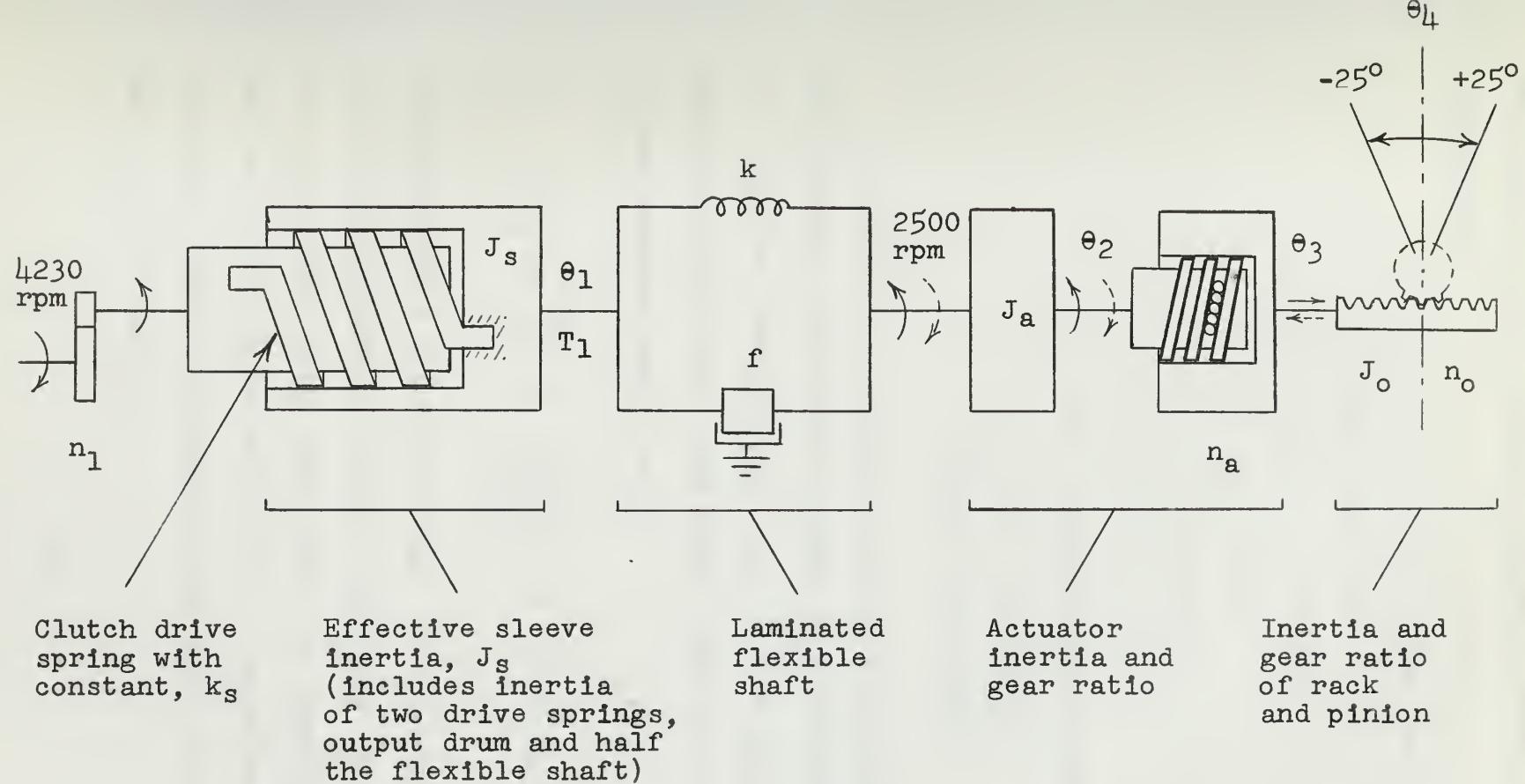
Figure 12. Block diagram showing mechanical features of system

The values of the various constants shown in Figure 12 are as follows:

$$n_1 = 1/1.69 \text{ (drive gear ratio)}$$

$$k_s = 5000 \text{ in-lb/rad}$$

$$J_s = 59 \times 10^{-6} \text{ in-lb-sec}^2$$

$$k = 261 \text{ in-lb/rad}$$

$$f = 1.3 \text{ in-lb/rad/sec}$$

$$J_a = 78 \times 10^{-6} \text{ in-lb-sec}^2$$

$$n_a = 1/86 \text{ (actuator gear ratio)}$$

$$J_o = 517.7 \times 10^{-3} \text{ in-lb-sec}^2$$

$$n_o = 1 \text{ (output gear ratio)}$$

It will now be shown that any contribution to the transfer function that would be made by the drive spring constant, k_s, and the inertia term, J_s, may be neglected. The frequency at which this term might begin to contribute to the system response would be at

$$\omega_s = \frac{k_s}{J_s} = \frac{5000}{59 \times 10^{-6}} = 9200 \text{ rad/sec} .$$

The anticipated frequency range of interest will extend only up to 300 radians per second, maximum. The frequency, ω_s, is so far above this range that its contribution to the system response will be negligible. Therefore, the term involving k_s and J_s will not be included in the derivation of the transfer function.

36

The equations of motion for the remaining elements shown in Figure 12 may be written as follows:

(1) $T_1 = f(\dot{\theta}_1 - \dot{\theta}_2) + k(\theta_1 - \theta_2)$

(2) $\theta_4 = n_o n_a \theta_2$

(3) $J'_o = \dfrac{1}{n_o^2 n_a^2} J_o$, where J'_o is the rack and

pinion inertia as seen at θ_2

(4) $f(\dot{\theta}_1 - \dot{\theta}_2) + k(\theta_1 - \theta_2) = J\ddot{\theta}_2$, where

$J = J_a + J'_o$

Solving equation (4) for initial conditions equal zero:

$$\ddot{\theta}_2 = \frac{f}{J}(\dot{\theta}_1 - \dot{\theta}_2) + \frac{k}{J}(\theta_1 - \theta_2)$$

$$\ddot{\theta}_2 + \frac{f}{J}\dot{\theta}_2 + \frac{k}{J}\theta_2 = \frac{f}{J}\dot{\theta}_1 + \frac{k}{J}\theta_1$$

$$(s^2 + \frac{f}{J} s + \frac{k}{J})\,\bar{\theta}_2 = (\frac{f}{J} s + \frac{k}{J})\,\bar{\theta}_1$$

$$\frac{\bar{\theta}_2}{\bar{\theta}_1} = \frac{\dfrac{f}{J} s + \dfrac{k}{J}}{s^2 + \dfrac{f}{J} s + \dfrac{k}{J}} = \frac{\dfrac{f}{k} s + 1}{\dfrac{J}{k} s^2 + \dfrac{f}{k} s + 1}$$

Evaluating the coefficients and factoring, the transfer function becomes

$$\frac{\bar{\theta}_2}{\bar{\theta}_1} = \frac{(\frac{1}{201}\, s + 1)}{(\frac{1}{205}\, s + 1)(\frac{1}{8555}\, s + 1)}$$

By including the runaway velocity, R , and the s in the denominator, the total transfer function, G_s , then becomes

$$G_s = \frac{175\,(\frac{1}{201}\, s + 1)}{s(\frac{1}{205}\, s + 1)(\frac{1}{8555}\, s + 1)}$$

Examining the significance of the various terms of this transfer function in the complex s-plane it is seen that the effect of the pole at s = -205 is nullified by a zero at s = -201 . And furthermore, since the frequency range of interest is restricted to values below 300 radians per second, the term involving the frequency of 8555 radians per second may be disregarded. The transfer function to be used in this analysis then is

$$G_s = \frac{175}{s}$$

Describing Function, G_d

The describing function was developed by Kochenburger as a means for analyzing a contactor servomechanism. Since the electromechanical spring clutch functions in the same

38

on-off manner as a three-position contactor, the describing function will be employed in the frequency response analysis of this paper.

The describing function, by definition, is the ratio of the amplitude of the fundamental component of the output of the nonlinearity, to the amplitude of the sinusoidal input to the nonlinearity. Having previously determined the characteristics of the clutch, they are shown schematically in Figure 13 for the purpose of establishing the notation which will be used in the development of the describing function. Δ signifies the width of the inactive zone, and h , the width of the hysteresis loop. The assumed input to the nonlinearity is the sinusoidal waveform of Figure 14(a). The resultant waveform of the correction signal is shown in Figure 14(b). Referring to these two figures, the describing function is now derived as follows:

$$\beta = \frac{1}{2} \left[\cos^{-1} \frac{\Delta - h}{2|E|} + \cos^{-1} \frac{\Delta + h}{2|E|} \right]$$

$$\alpha = \frac{1}{2} \left[\cos^{-1} \frac{\Delta - h}{2|E|} - \cos^{-1} \frac{\Delta + h}{2|E|} \right]$$

By means of a Fourier analysis, the magnitude of the fundamental component of the correction signal, $\left| N_1 \right|$ may be shown to be

$$\left| N_1 \right| = \frac{2}{\pi} \sqrt{4 \sin^2 \beta} = \frac{4}{\pi} \sin \beta$$
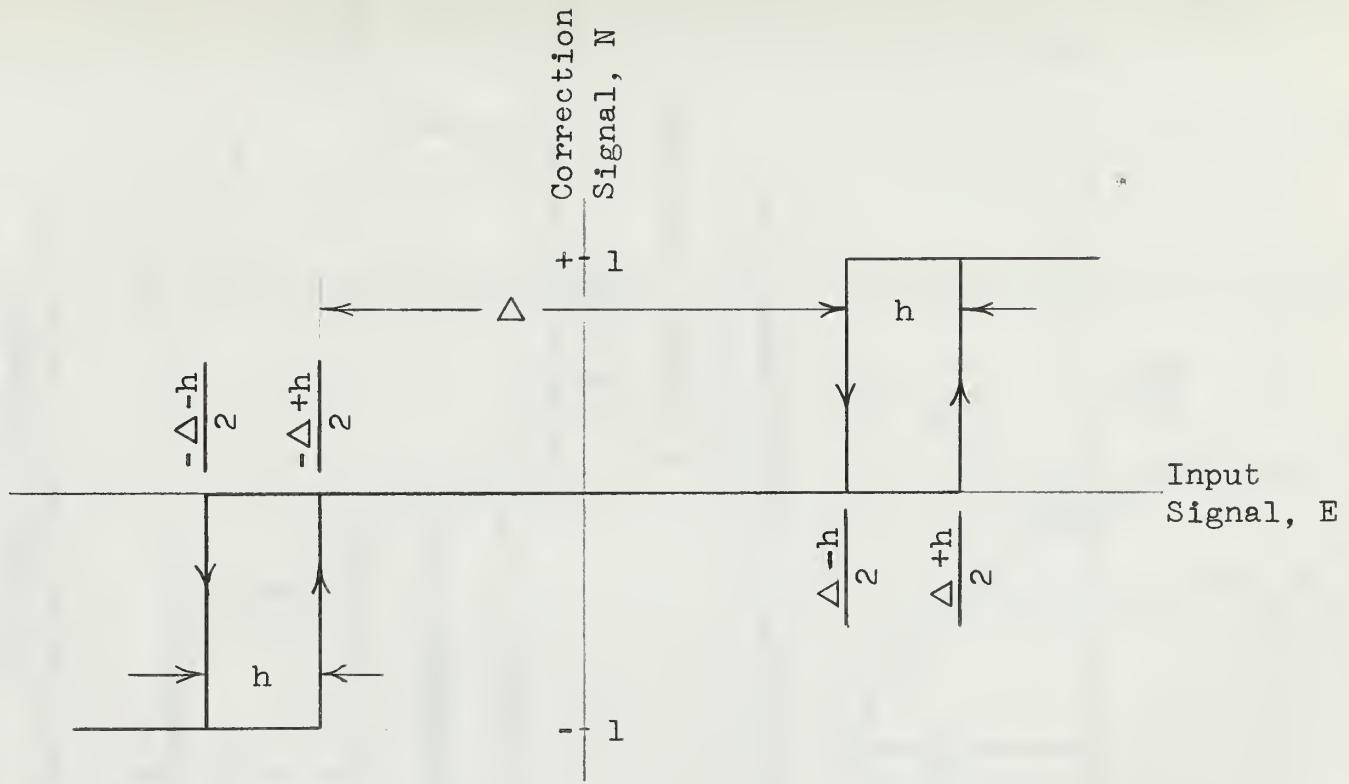
Figure 13. On-off characteristics of clutch
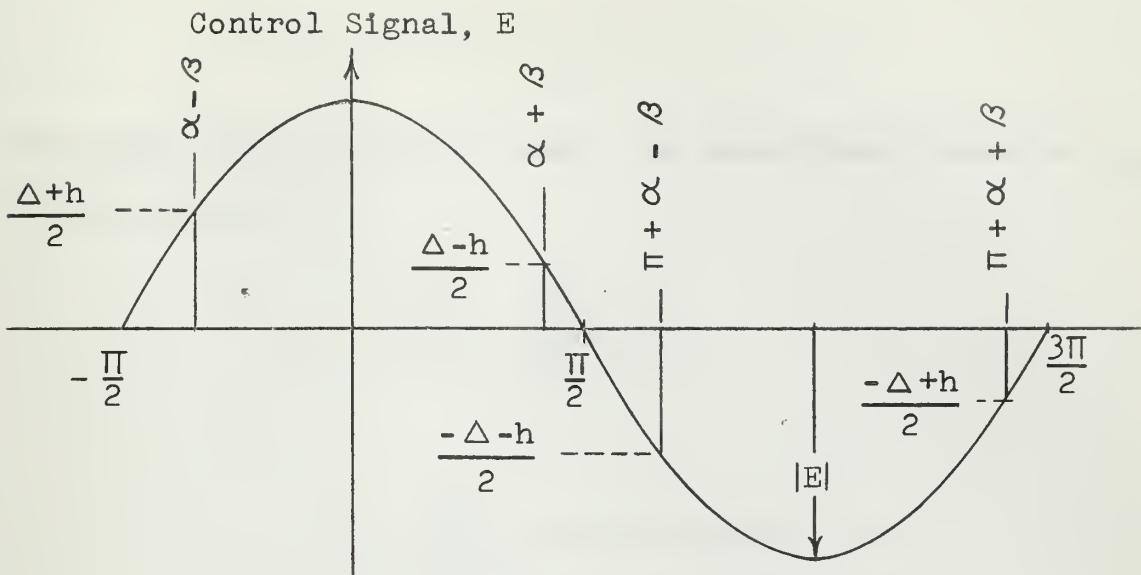
(a)   Assumed input to nonlinearity
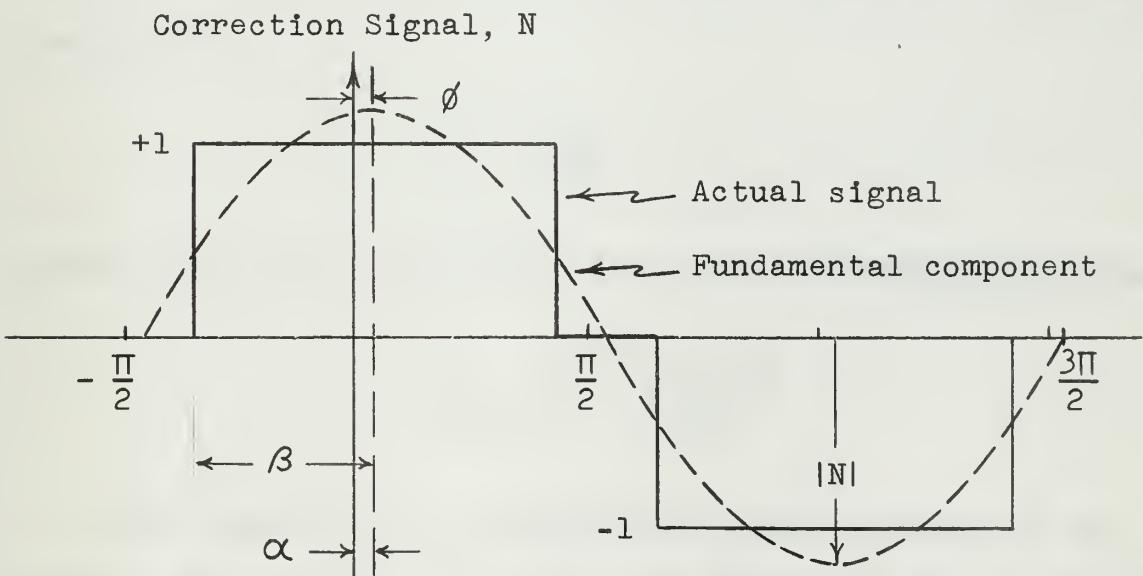
(b)   Output of nonlinearity and its
      fundamental component

Figure 14.   Relationship of correction signal to control
             signal for on-off system possessing both an
             inactive zone and hysteresis

41

and the phase angle, ϕ, is seen in Figure 14(b) to be

$$\phi = -\alpha,$$

the minus sign indicating lag. The describing function, G_d is now written as

$$G_d = \frac{N_1}{E} = \left|\frac{N_1}{E}\right| \underline{/\phi}$$

$$= \frac{4}{\pi|E|} \sin \beta \underline{/-\alpha}$$

For the case of no hysteresis, the phase angle is zero, and β simplifies to

$$\beta = \cos^{-1} \frac{\Delta}{2|E|}$$

giving the rather simplified form of the describing function,

$$G_d = \frac{4}{\pi|E|} \sqrt{1 - \left(\frac{\Delta}{2|E|}\right)^2}$$

This completes the mathematical representation of the system. The transfer function, the describing function and the transportation lag are all that is needed to proceed with the mathematical analysis of the closed-loop system.

CHAPTER VI

CLOSED-LOOP RESPONSE OF THE SYSTEM

Analytic Development

The closed-loop frequency response of a nonlinear system often is not easy to determine. Difficulties arise because for a given system input and frequency the amplitude of the actuating signal, E , depends on G_d , but G_d is in turn determined by E . As a result of this interdependence of G_d and E , the calculation of the closed-loop frequency response for a given input is at times a rather complicated procedure. In solving the problem this analysis makes use of an approach which is attributed to E. Levinson [3]. A graphical technique is used in determining values of E which satisfy both frequency and nonlinear conditions. The details are explained in the development which follows.

Referring to Figure 11, an equation for the error signal, E is derived

$$E = \theta_i - \theta_o \tag{1}$$

$$\theta_o = E\, G_d G_s \in ^{-st}$$

$$E = \theta_i - E\, G_d G_s \in ^{-st}$$

$$= \frac{\theta_i}{1 + G_d G_s \in ^{-st}} \tag{2}$$

43

Recalling

$$G_d = \frac{4}{\pi |E|} \sin \beta \,\underline{/-\alpha}$$

let

$$\frac{4}{\pi |E|} \sin \beta = N$$

then

$$G_d = N \cos \alpha - jN \sin \alpha$$

also recalling

$$G_s = \frac{175}{s}$$

Since it is the frequency response which is of interest, a substitution $s = j\omega$ is made, giving

$$G_s = \frac{175}{j\omega}$$

Similarly for the transportation lag,

$$\epsilon^{-st} = \epsilon^{-j\omega t} = \epsilon^{-j\phi_1} , \text{ where } \phi_1 = \omega t$$

$$= \cos \phi_1 - j \sin \phi_1$$

Making the substitutions equation (2) now becomes

$$E = \frac{\theta_i}{1 + \left[N \cos \alpha - jN \sin \alpha \right] \left[\frac{175}{j\omega} \right] \left[\cos \phi_1 - j \sin \phi_1 \right]} \quad (3)$$

$$E = \frac{\theta_i\,(j\omega)}{j\omega + 175N\left[(\cos\alpha\ \cos\emptyset_1 - \sin\alpha\ \sin\emptyset_1) - j(\cos\alpha\ \sin\emptyset_1 + \sin\alpha\ \cos\emptyset_1)\right]}$$

$$= \frac{\theta_i\,(j\omega)}{j\omega + 175N\left[\cos(\alpha + \emptyset_1) - j\sin(\alpha + \emptyset_1)\right]}$$

$$= \frac{\theta_i\,(j\omega)}{\left[175N\cos(\alpha + \emptyset_1)\right] + j\left[\omega - 175N\sin(\alpha + \emptyset_1)\right]} \tag{4}$$

The magnitude of the error may then be written as

$$\tag{5}$$
$$|E| = \frac{|\theta_i|\,\omega}{\left[\left[175N\cos(\alpha + \emptyset_1)\right]^2 + \left[\omega - 175N\sin(\alpha + \emptyset_1)\right]^2\right]^{\frac{1}{2}}}$$

Squaring both sides of equation (5),

$$\tag{6}$$
$$|E|^2 = \frac{|\theta_i|^2\,\omega^2}{\left[175N\cos(\alpha + \emptyset_1)\right]^2 + \left[\omega - 175N\sin(\alpha + \emptyset_1)\right]^2}$$

or,

$$|E|^2\left[175N\cos(\alpha + \emptyset_1)\right]^2 + |E|^2\left[\omega - 175N\sin(\alpha + \emptyset_1)\right]^2 = |\theta_i|^2\,\omega^2$$

transposing terms,

45

$$|E|^2 \left[175N \cos(\alpha + \emptyset_1)\right]^2$$
$$= |\theta_i|^2 \omega^2 - |E|^2 \left[\omega - 175N \sin(\alpha + \emptyset_1)\right]^2 \qquad (7)$$

Taking the square root of equation (7),

$$|E| \left[175N \cos(\alpha + \emptyset_1)\right]$$
$$= \left[|\theta_i|^2\omega^2 - |E|^2 \left[\omega - 175N \sin(\alpha + \emptyset_1)\right]^2\right]^{\frac{1}{2}} \qquad (8)$$

Rearranging terms and factoring, equation (8) may be expressed in the form

$$(9)$$
$$|NE| = \frac{\omega}{175 \cos(\alpha + \emptyset_1)} \left[|\theta_i|^2 - |E|^2 \left[1 - \frac{175N}{\omega} \sin(\alpha + \emptyset_1)\right]^2\right]^{\frac{1}{2}}$$

Now, since the input to the system is assumed to be sinusoidal

$$\theta_i = A \sin \omega t$$

therefore, $|\theta_i|^2 = A^2$.

Making this substitution, equation (9) becomes

$$(10)$$
$$|NE| = \frac{\omega}{175 \cos(\alpha + \emptyset_1)} \left[A^2 - |E|^2 \left[1 - \frac{175N}{\omega} \sin(\alpha + \emptyset_1)\right]^2\right]^{\frac{1}{2}}$$

Each side of equation (10) is evaluated separately. A width of inactive zone, $\triangle$, is first chosen. For the example

whose results are plotted in Figure 15, a value of $\triangle = 2.01^{\circ}$ was selected. Preliminary equipment tests indicated an essentially constant value of the ratio $h/\triangle = 0.091$. Thus, for the selected value of $\triangle$, $h = 0.183^{\circ}$. The left side of equation (10) is now evaluated, letting $|E|$ vary over the anticipated range of error signal. The results are plotted in Figure 15 as the $|NE|$ curve.

To evaluate the right-hand side of equation (10), the value of $\triangle$ remains unchanged. A magnitude of input to the system is next chosen. For the example whose results are plotted in Figure 15, $A = 10.7^{\circ}$. There still remain two variables, ω and $|E|$, in this part of the equation. The next step is to select a value of ω, then letting $|E|$ vary over a sufficient range, a curve is obtained which is also plotted in Figure 15 and labeled with its associated value of ω, say $\omega = 2\pi$. Another value of ω is selected and the procedure is repeated yielding another curve, say the $\omega = 4\pi$ curve of Figure 15. This procedure is repeated until the complete frequency range of interest has been covered.

The points of intersection of the $|NE|$ curve with the ω_i curves yield values of $|E|$ which satisfy equation (10) and thus satisfy both frequency and nonlinear conditions. Having determined values of N and $|E|$ over the desired frequency range the magnitude of the system output is known from the relationship

47
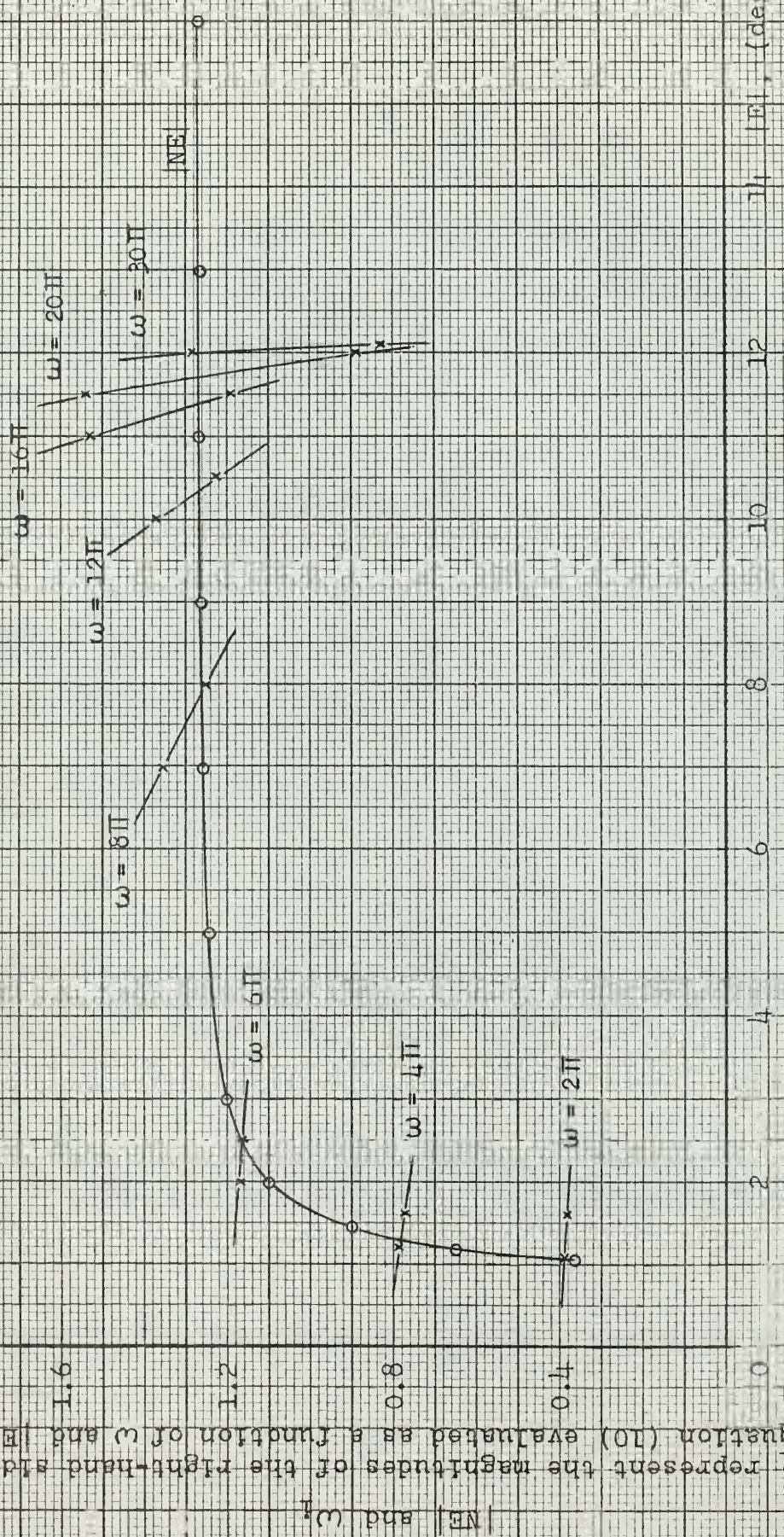
Figure 15. Graphical solution to equation (10) for determination of closed-loop gain and phase ($A = 10.7°$, $\Delta = 2.010$, $h/\Delta = 0.091$)

$$\theta_o \;=\; \left|\mathrm{E}\right| \left|\mathrm{G_d}\right| \left|\mathrm{G_s}\right| \tag{11}$$

$$=\; \left|\mathrm{NE}\right| \frac{175}{\omega} \tag{12}$$

Since it is common practice to express the closed-loop response in form of gain and phase versus frequency, the gain equation is obtained by dividing equation (12) by the magnitude of the input,

$$\left|\frac{\theta_o}{\theta_i}\right| \;=\; \left|\mathrm{NE}\right| \frac{175}{\omega A} \tag{13}$$

Similarly, the phase of $\dfrac{\theta_o}{\theta_i}(j\omega)$ may be obtained. Looking at the equation for this ratio

$$\frac{\theta_o}{\theta_i}(j\omega) \;=\; \frac{\mathrm{E}\ \mathrm{G_d}\mathrm{G_s}\, \in^{-j\omega t}}{\theta_i} \tag{14}$$

$$=\; \frac{\theta_i(j\omega)\ N\ \underline{/-\alpha}\ \dfrac{175}{(j\omega)}\ 1\ \underline{/-\phi_1}}{\theta_i\left[\left[175N\cos(\alpha+\phi_1)\right] + j\left[\omega - 175N\sin(\alpha+\phi_1)\right]\right]}$$

$$\tag{15}$$

$$=\; \frac{175N\ \underline{/-\alpha-\phi_1}}{\left[175N\cos(\alpha+\phi_1)\right] + j\left[\omega - 175N\sin(\alpha+\phi_1)\right]}$$

From equation (15) the phase of $\dfrac{\theta_o}{\theta_i}(j\omega)$, which is denoted by ϕ is

49

$$\emptyset = - \left[\alpha + \emptyset_1 + \tan^{-1} \frac{\left[\omega - 175N \sin(\alpha + \emptyset_1) \right]}{\left[175N \cos(\alpha + \emptyset_1) \right]} \right] \quad (16)$$

With the aid of Figure 15, equation (16) may be evaluated to give the desired phase versus frequency plot.

Comparison of Analytic and Equipment Results

The gain curve obtained from evaluating equation (13) for the assumed values of θ_i and $\triangle$ is plotted in Figure 16(a). For ease of comparison, on the same plot is shown the corresponding curve obtained from an equipment run utilizing the same parameters. It will be noted that the analytic and equipment gain curves compare quite favorably over the entire frequency range.

The phase results which were obtained from the evaluation of equation (16) are plotted in Figure 16(b). Here the analytic approach gives extremely close correlation with equipment results up to a frequency of approximately 100 radians per second, beyond which the two curves begin to diverge slightly. Nevertheless, the two curves compare reasonably well over the entire frequency range.

For an input, $\theta_i = 10.7^\circ \sin \omega t$ and an inactive zone, $\triangle = 2.01^\circ$, Figure 16(a) indicates the gain response of the system to be essentially flat until velocity saturation occurs at about 20 radians per second. The system bandwidth for the given conditions is approximately five cycles per second.
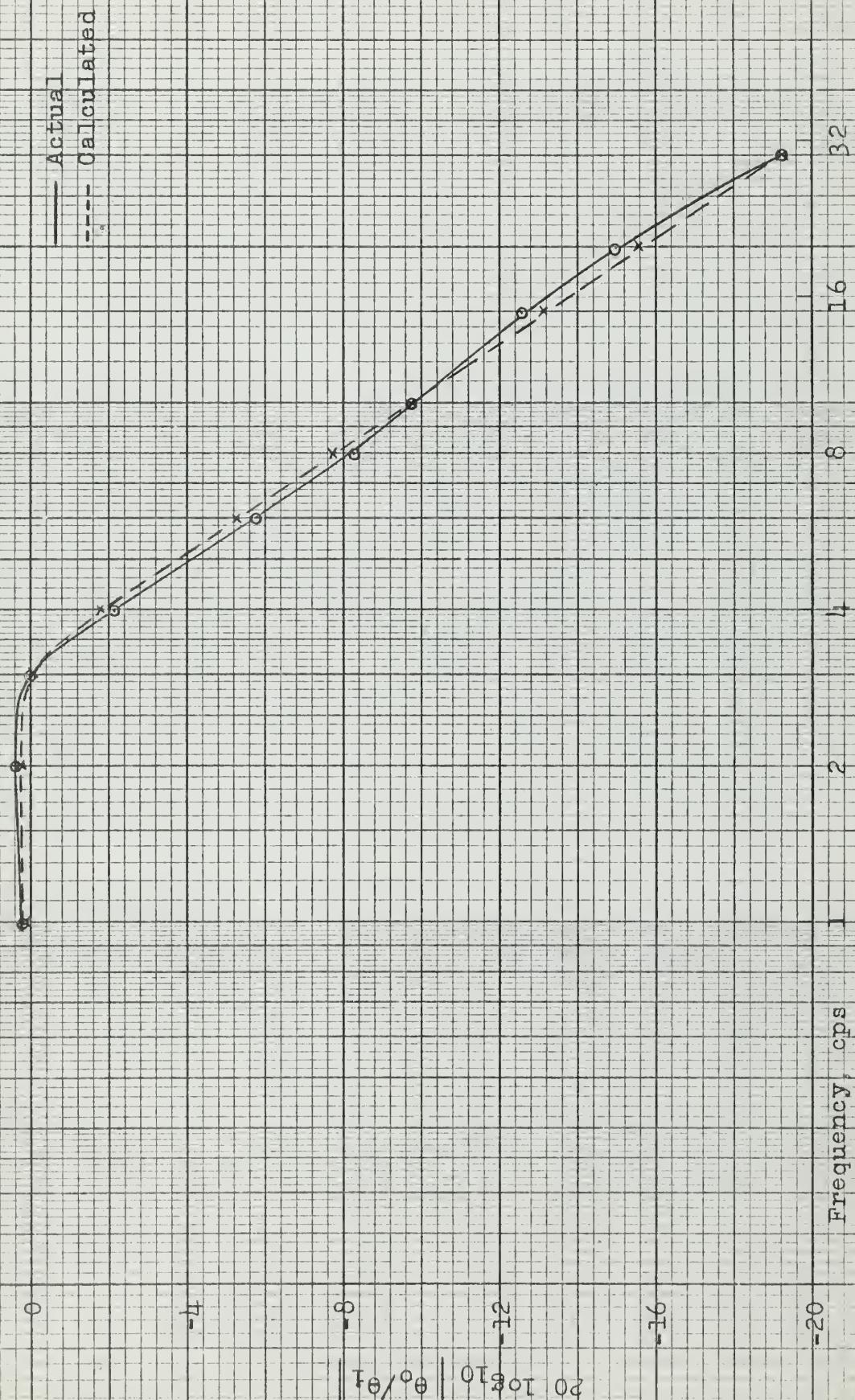
Figure 16(a). Actual and calculated closed-loop gain for 10.7° input and 2.01° inactive zone width

Figure 16(b). Actual and calculated closed-loop phase versus frequency for 10.7° input and 2.01° inactive zone width
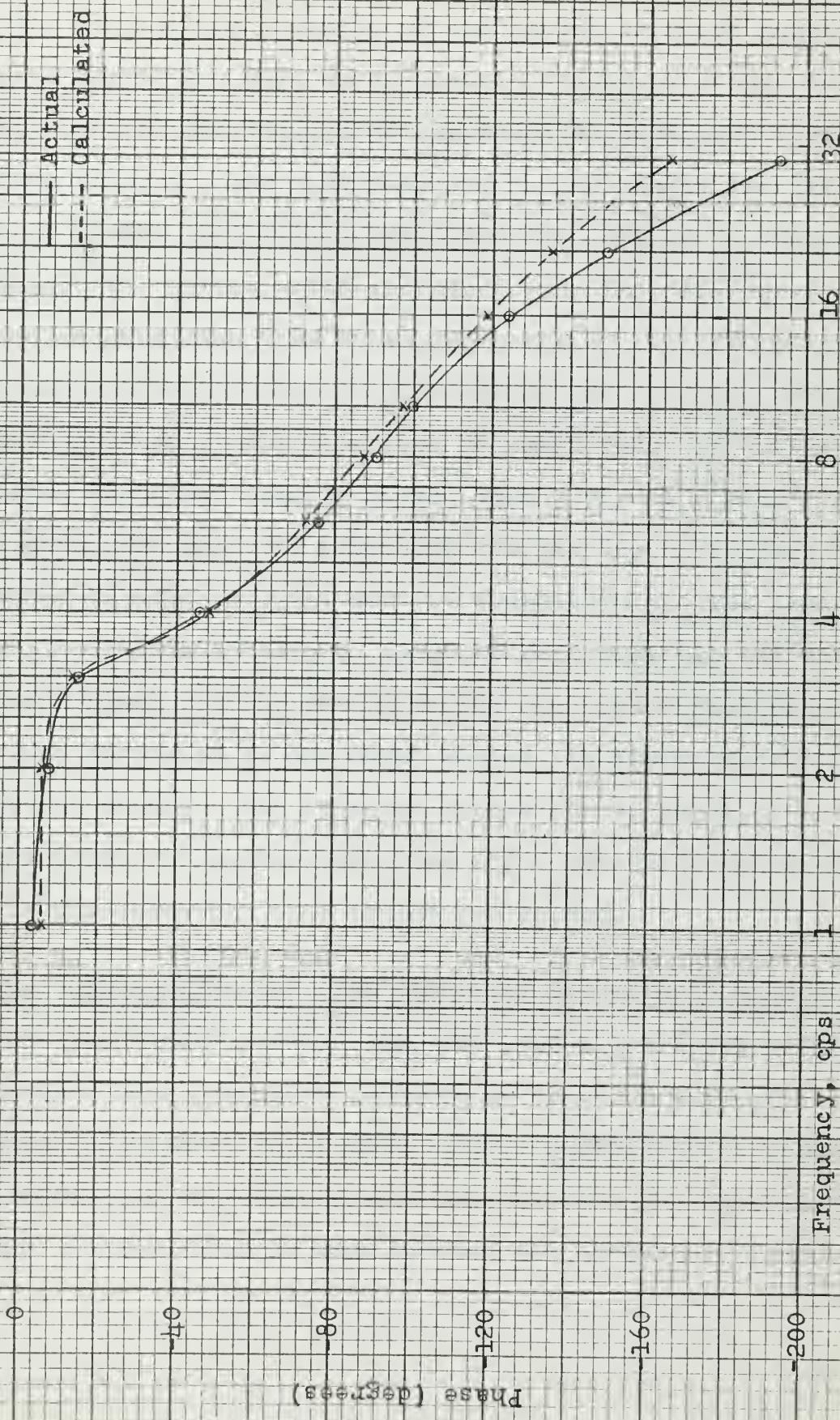
Response to Other Amplitudes of Input

The closed-loop response of the system to other magnitudes of input, A , were calculated by the above method for comparison with the results obtained on the equipment. The inactive zone, $\triangle$, was maintained at 2.01°. While the |NE| curve of Figure 15 is still applicable so long as $\triangle$ remains unchanged, the curves which intersect with the |NE| curve must be recalculated each time a new magnitude of θ_i is chosen. This means re-evaluating the right-hand side of equation (10), for each new θ_i . This was done for magnitudes of θ_i above and below the first example given, namely for A = 21.4° and A = 5.35°. The gain and phase results for θ_i = 21.4°sin ωt are shown in Figures 17(a) and (b) respectively. The same close correlation is seen to exist between analytic and actual equipment results. The bandwidth for the higher magnitude of input has decreased as one might expect, to approximately 2.5 cycles per second. The response curves for an input of 5.35° are presented in Figures 18(a) and (b). The bandwidth in this case is approximately nine cycles per second.

Response without Reverse Kick Generator and with $\triangle = 4.9°$

The gain and phase loci for the system operating without the reverse kick generator and with an inactive zone of 4.9° are shown in Figures 19(a) and (b). To emphasize the true significance of the reverse kick generator in the amplifier circuit, a comparison is made between the curves of Figures

53
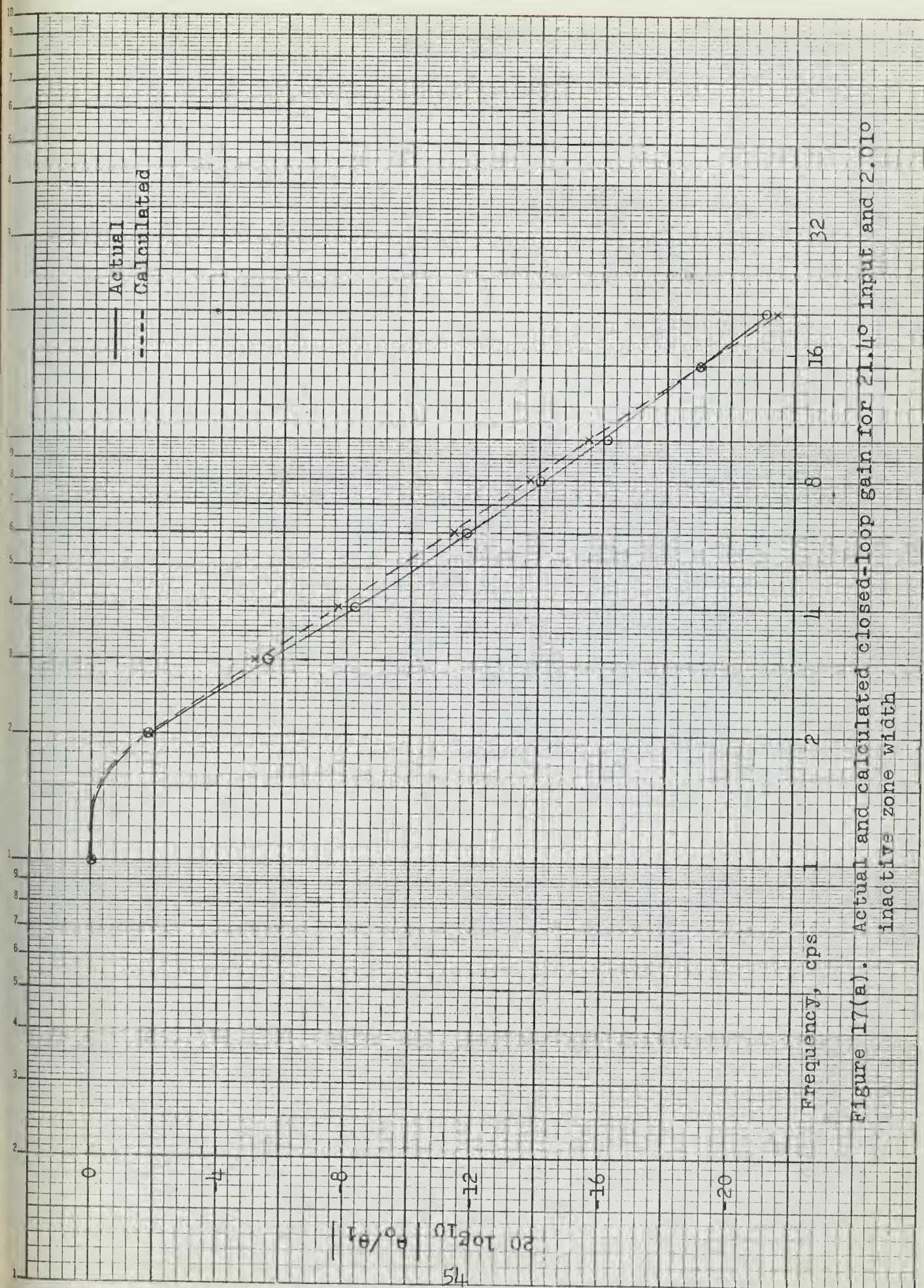
Figure 17(a). Actual and calculated closed-loop gain for 21.4° input and 2.010 inactive zone width

Figure 17(b). Actual and calculated closed-loop phase versus frequency for 21.4° input and 2.01° inactive zone width
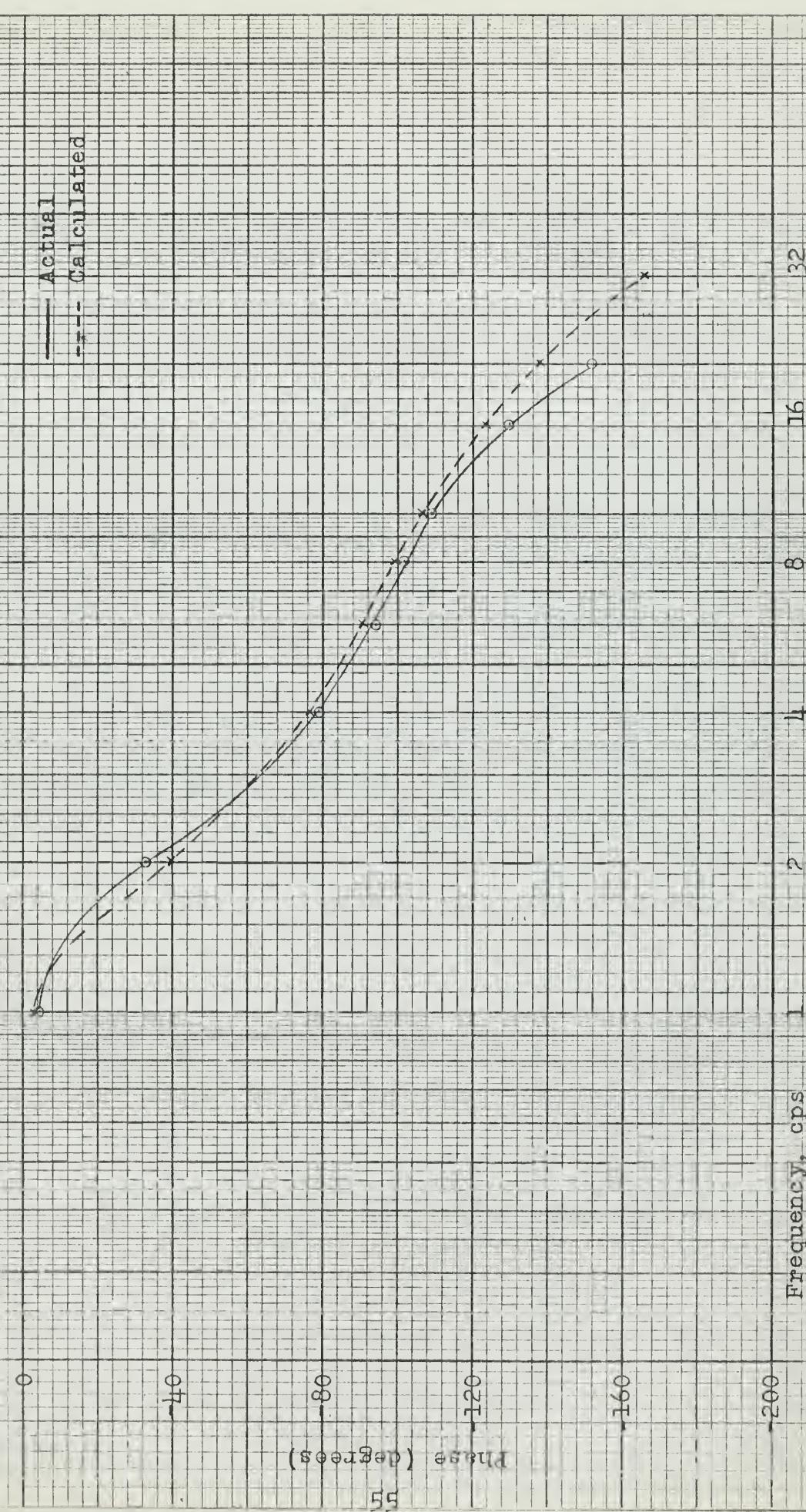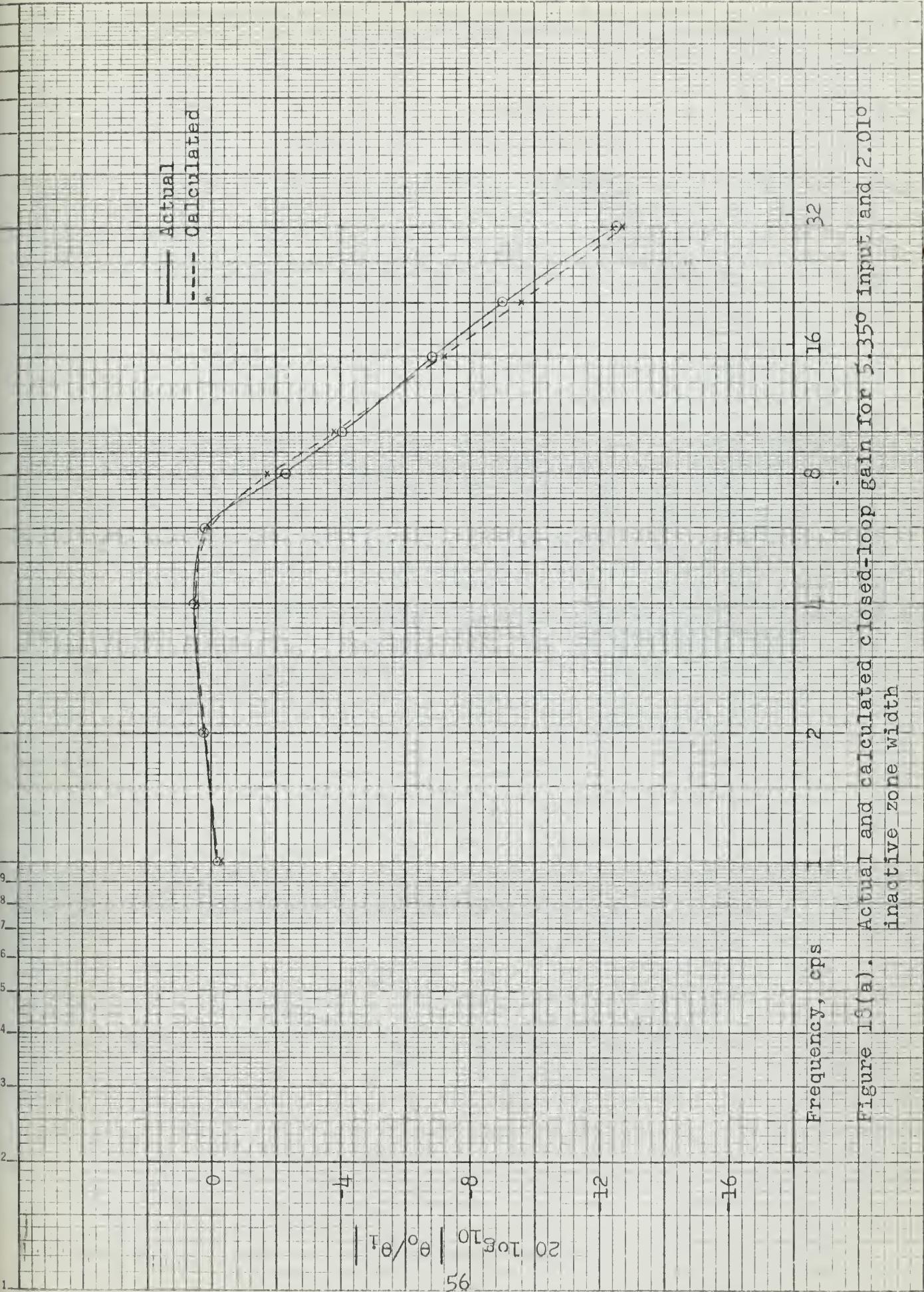
Figure 13(a). Actual and calculated closed-loop gain for 5.35° input and 2.010° inactive zone width

Figure 18(b). Actual and calculated closed-loop phase versus frequency for 5.35° input and 2.01° inactive zone width
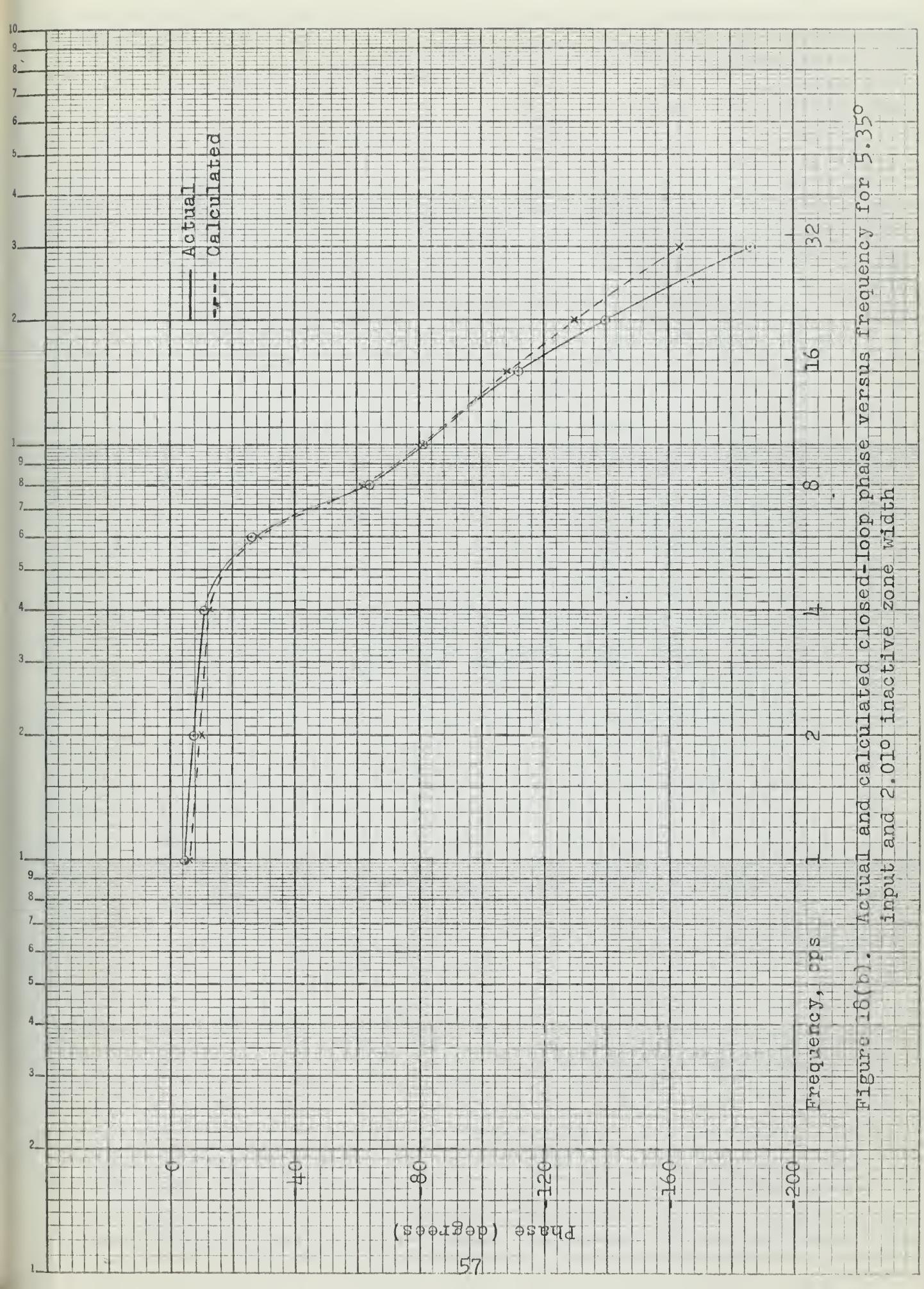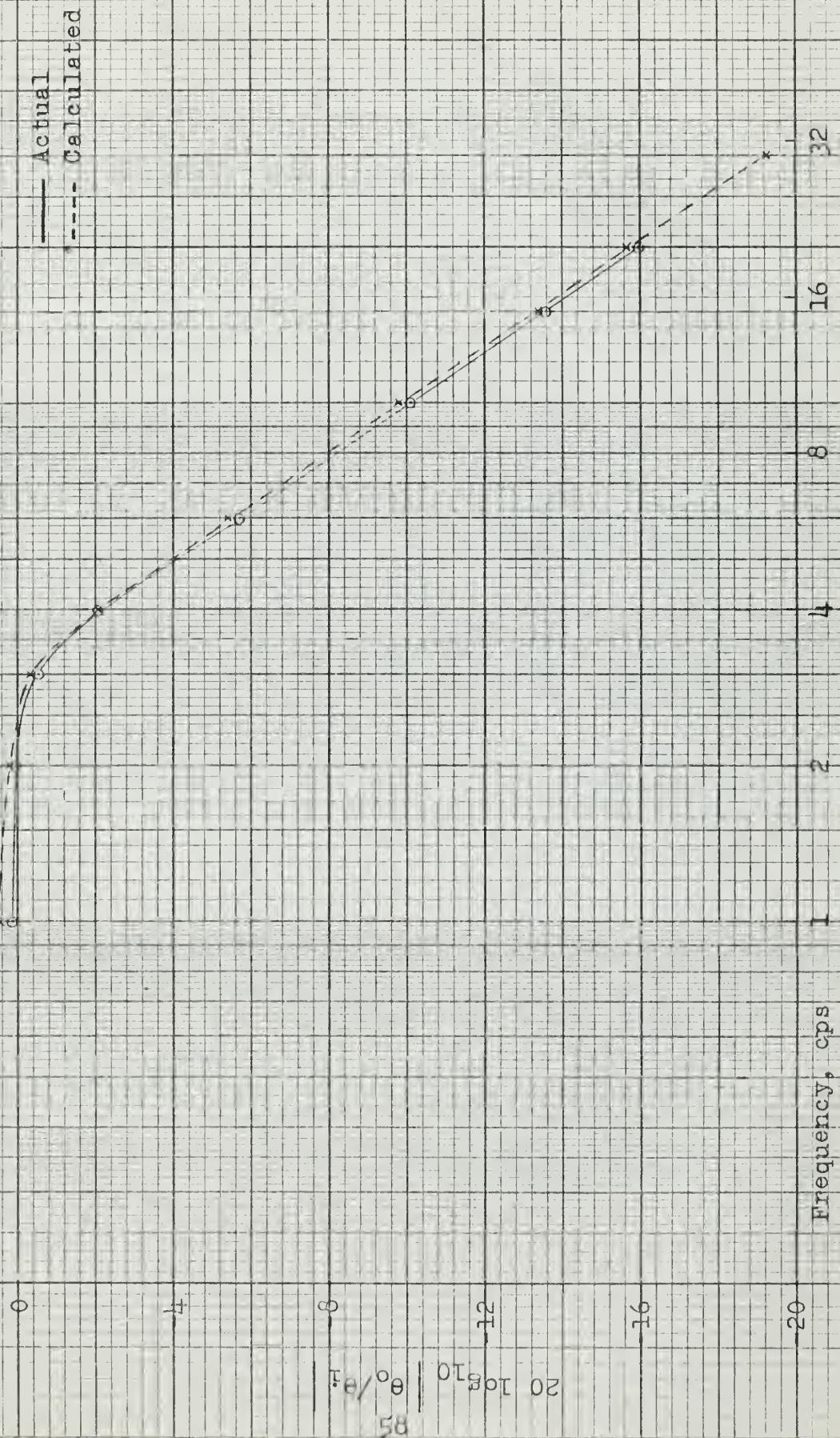
Figure 19(a). Actual and calculated closed-loop gain for 10.7° input, 4.90 width of inactive zone, and no reverse-kick generator

Frequency, cps

$20 \log_{10} |\theta_o/\theta_i|$

59

Figure 19(b). Actual and calculated closed-loop phase versus frequency for 10.7° input, 4.9° width of inactive zone, and no reverse-kick generator.
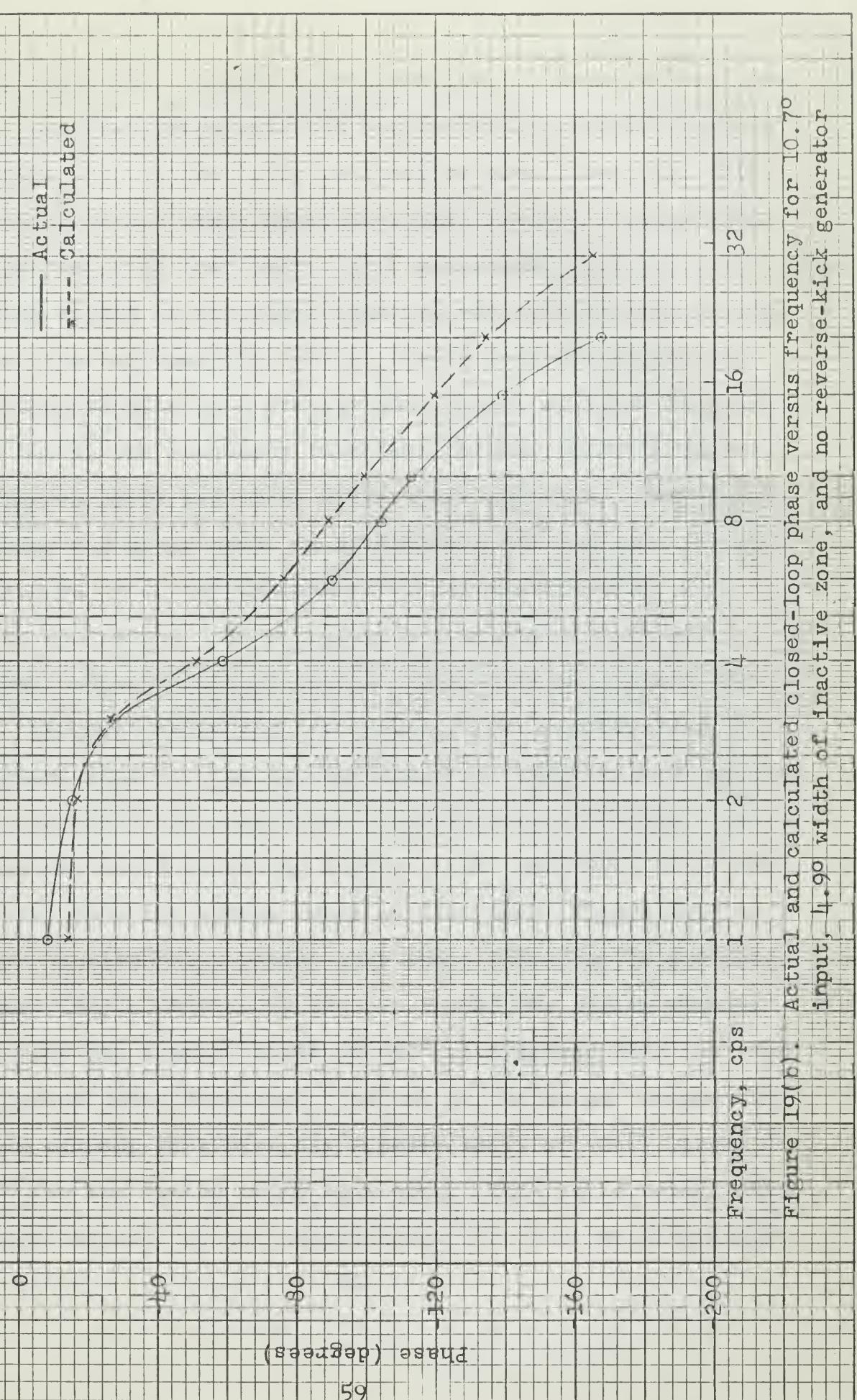
16(b) and 19(b). Figure 19(b) is a plot of phase versus frequency of the system with the reverse kick generator removed from the circuit and using an inactive zone, $\Delta = 4.9°$. Figure 16(b) on the other hand shows phase versus frequency for the system using the reverse kick generator, but with $\Delta = 2.01°$. Now the effect of the wider inactive zone may be seen by comparing the two analytic curves. It is seen the wider inactive zone results in a greater phase shift at lower frequencies but as the frequency increases the two analytic curves of Figures 16(b) and 19(b) differ less and less. Practically speaking the phase shift is essentially the same for the two magnitudes of Δ for frequencies above approximately four cycles per second. At 20 cycles per second, for example, both analytic curves indicate a phase shift of approximately 135° lag. Theoretically then, the phase shift observed from the equipment runs for the two magnitudes of inactive zone should be essentially the same beyond four cycles per second. Comparing the solid curves of Figures 16(b) and 19(b) it is seen, however, that the system using no kick-back (Figure 19b) is lagging considerably behind that where kick-back is employed, (Figure 16b). At four cycles per second the system without kick-back has a phase shift of -59° as compared with -46° for the system using kick-back. And at 20 cycles per second the system without kick-back has a phase shift of -168° versus -150° for the system using kick-back. This is certainly sufficient evidence of the importance of the reverse kick genera-

tor in improving the system response.

The response gain curve for the system using the wider inactive zone and no kick-back is shown in Figure 19(a). It is interesting to note, however, that the gain or magnitude results shown in this figure are essentially the same as those obtained for the system using kick-back and an inactive zone, $\Delta = 2.01°$ (Figure 16a).

Typical Response of the System to a Sinusoidal Input

In the previous sections response gain and phase characteristics have been discussed at some length. To supplement this discussion it seems appropriate to show some representative examples of the system response to an applied sinusoidal input signal. In Figures 20(a), (b), (c), and (d) are shown the response to an input, $\theta_i = 10.7° \sin \omega t$ for frequencies from one cycle per second to six cycles per second. In Figures 21(a), (b), (c), and (d) are shown similar curves for an input, $\theta_i = 21.4° \sin \omega t$. The width of the inactive zone is $2.01°$ for both sets of curves.
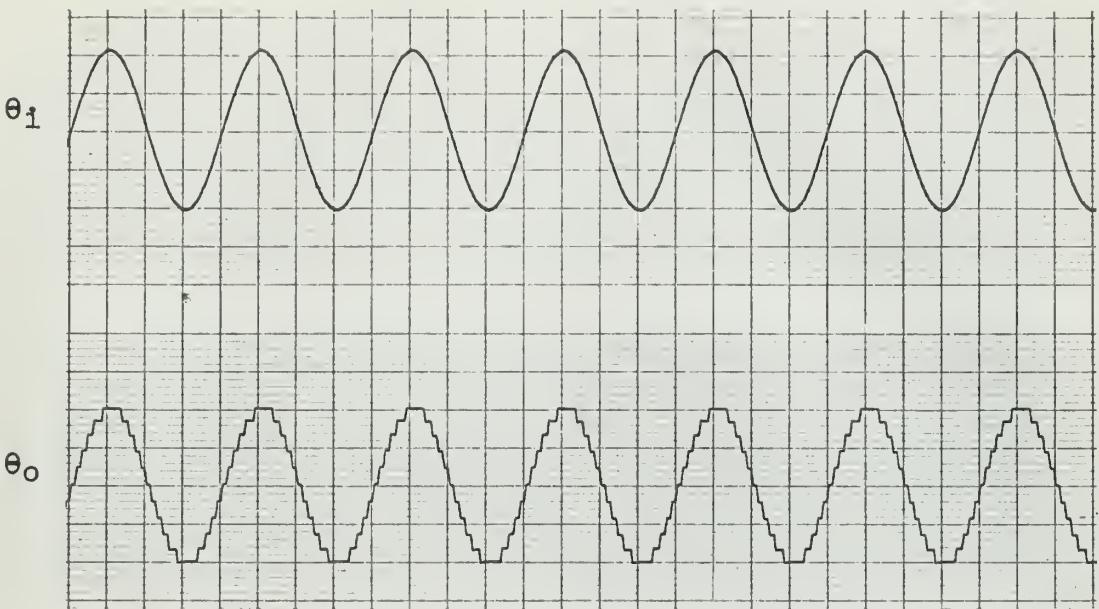
(a) Frequency of one cycle per second
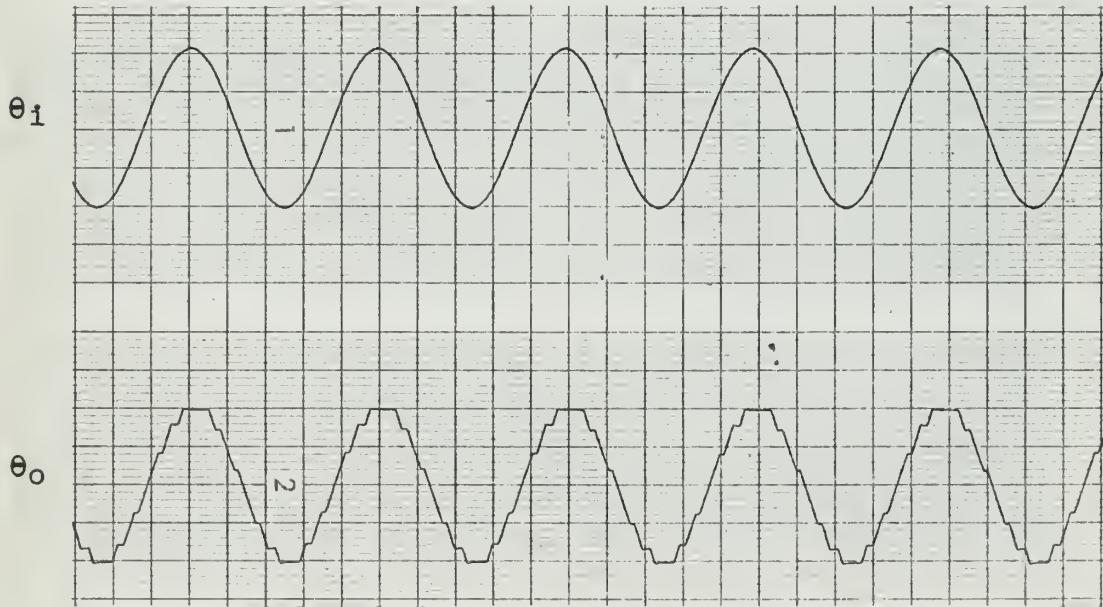
(b) Frequency of two cycles per second

Figure 20. Typical response curves for a sinusoidal
input of amplitude 10.7° ($\triangle$ = 2.01°)
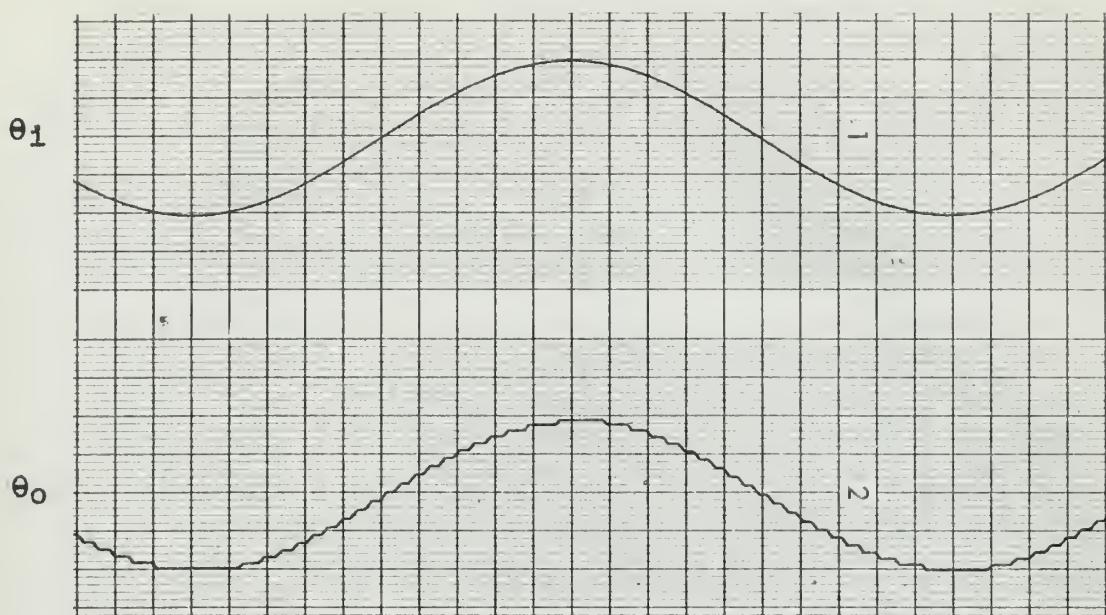
(a) Frequency of one-half cycle per second
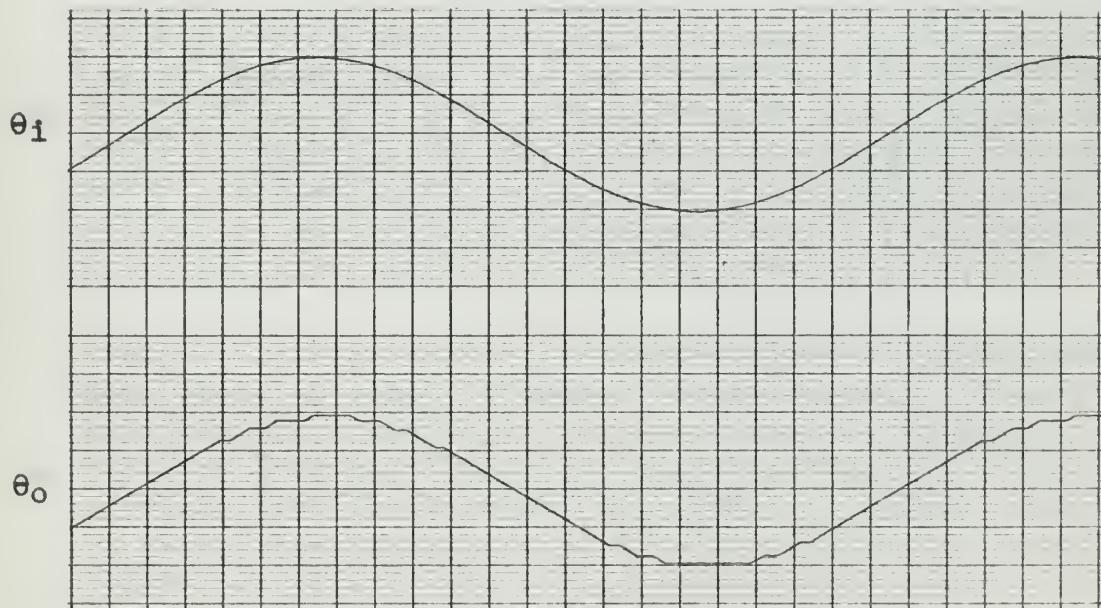
(b) Frequency of one cycle per second

Figure 21. Typical response curves for a sinusoidal
input of amplitude $21.4°$ ($\triangle = 2.01°$)
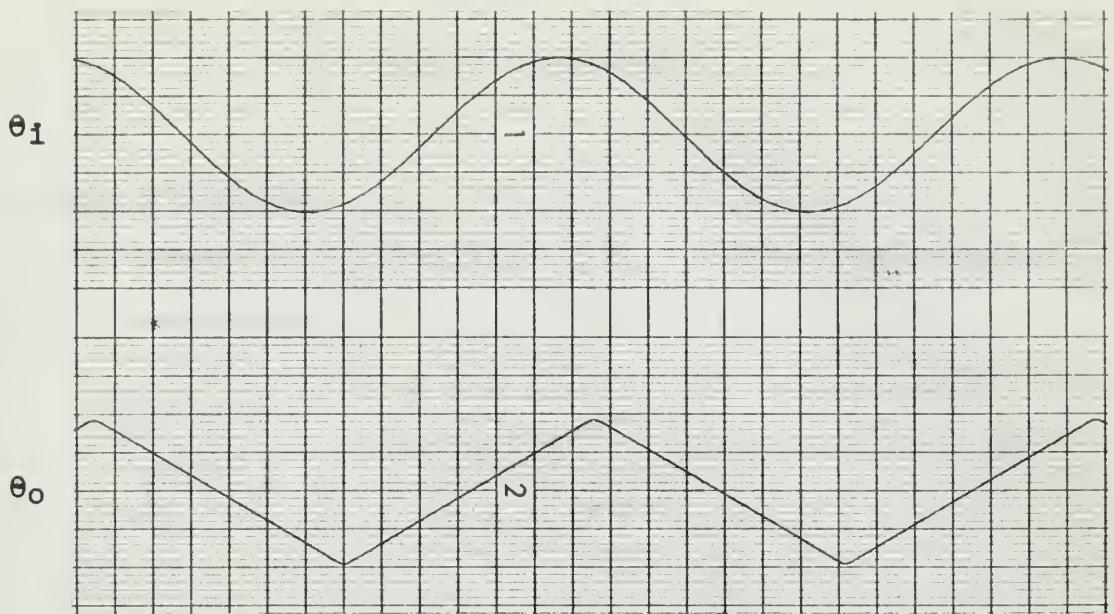
(c)   Frequency of 1.5 cycles per second
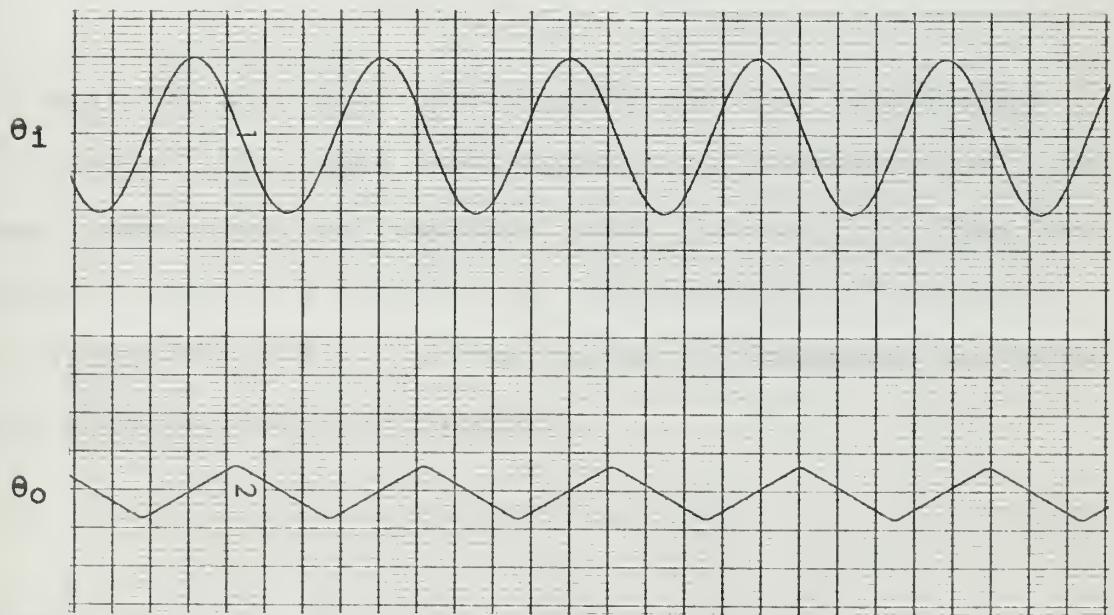
(d)   Frequency of four cycles per second

Figure 21.   Typical response curves for a sinusoidal
input of amplitude 21.4° ($\triangle = 2.01^\circ$)
Continued

65

CHAPTER VII

SYSTEM STABILITY

Absolute Stability

To examine the stability of the system, the response ratio is expressed as

$$\frac{\theta_o}{\theta_i}(j\omega) = \frac{G_d G_s \epsilon^{-j\omega t}}{1 + G_d G_s \epsilon^{-j\omega t}}$$

$$= \frac{G_d}{G_s^{-1} \epsilon^{j\omega t} + G_d} \tag{17}$$

The test for stability depends only upon the denominator of equation (17) since the numerator is independent of frequency and merely represents a scale factor [2]. Thus the study of stability involves an investigation of the poles of $G_s^{-1} \epsilon^{j\omega t} + G_d$, or the values of frequency and amplitude which satisfy the equation

$$G_s^{-1} \epsilon^{j\omega t} = -G_d \tag{18}$$

Substituting for the inverse transfer function, G_s^{-1} , equation (18) becomes

$$\frac{j\omega \; \epsilon^{j\omega t}}{175} = -G_d \tag{19}$$

66

Now the procedure is to plot each side of equation (19) separately for the purpose of analyzing system stability. In the preliminary analysis the value of t in equation (19) was determined to be seven milliseconds. Using this value, the left-side of equation (19), which shall be referred to as the frequency locus, is plotted in Figure 22 for values of ω up to 300 radians per second. For purposes of illustration, the value of $\triangle$ = 2.01° which was used in the closed-loop analysis of chapter VI is assumed in evaluating the right-hand side of equation (19). The latter, which shall be referred to as the amplitude locus, is also shown on the Nyquist plot of Figure 22. The points along the amplitude locus represent the magnitude of the error signal which is really the input to the nonlinear clutch. The relative orientation of the amplitude and frequency loci determines the stability characteristics of the system. Since the amplitude locus always appears to the left of an observer as he traverses the frequency locus in the direction of increasing frequency the system will be stable for all amplitudes of input. Suppose now, the amplifier gain is increased until the corresponding width of inactive zone is 0.962°. The corresponding amplitude and frequency loci are plotted in Figure 23. The frequency locus, of course, is identical to that of Figure 21, however the amplitude locus is changed until it now intersects the frequency locus at two points. System
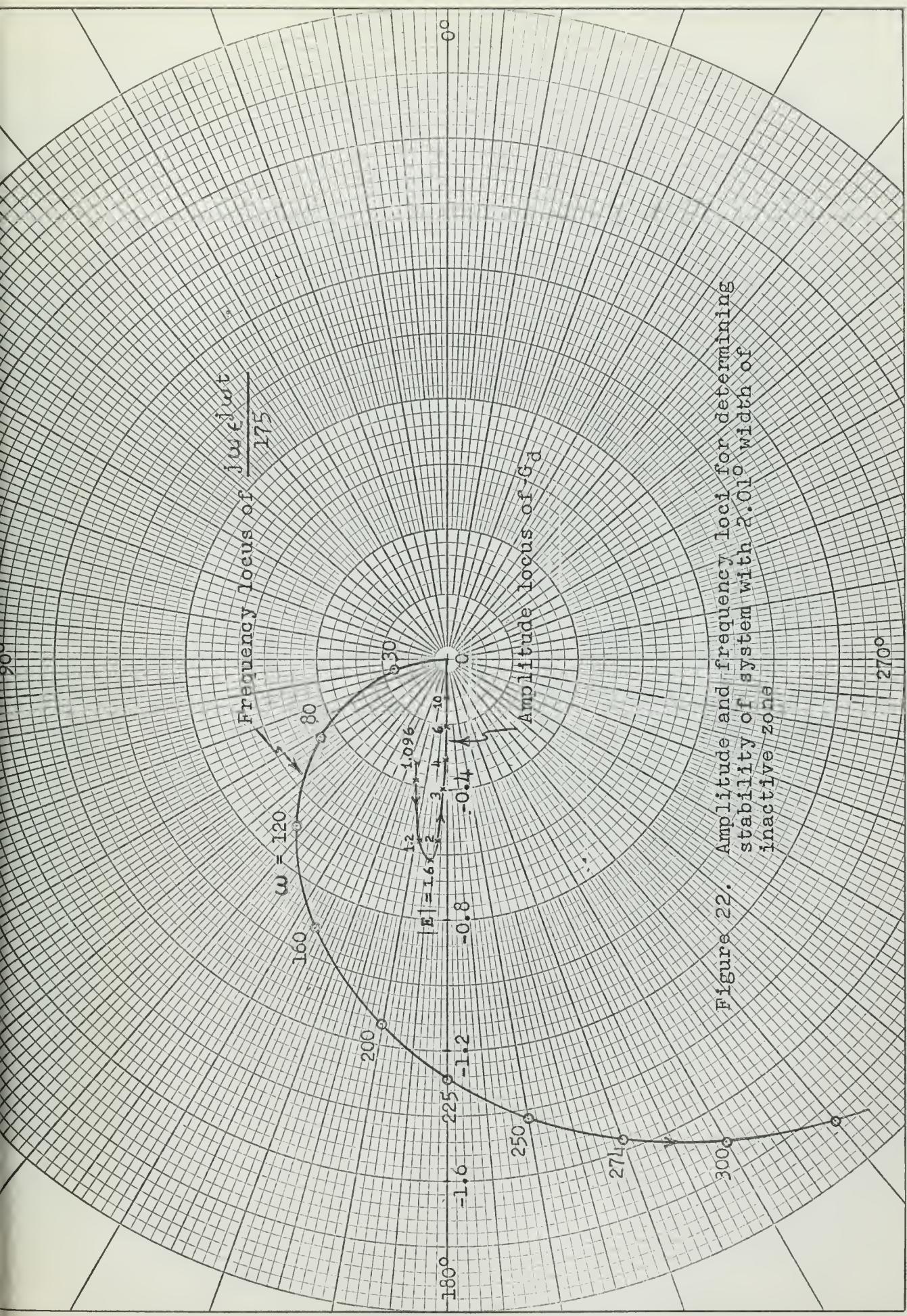
67

Figure 22. Amplitude and frequency loci for determining stability of system with 2.0° width of inactive zone
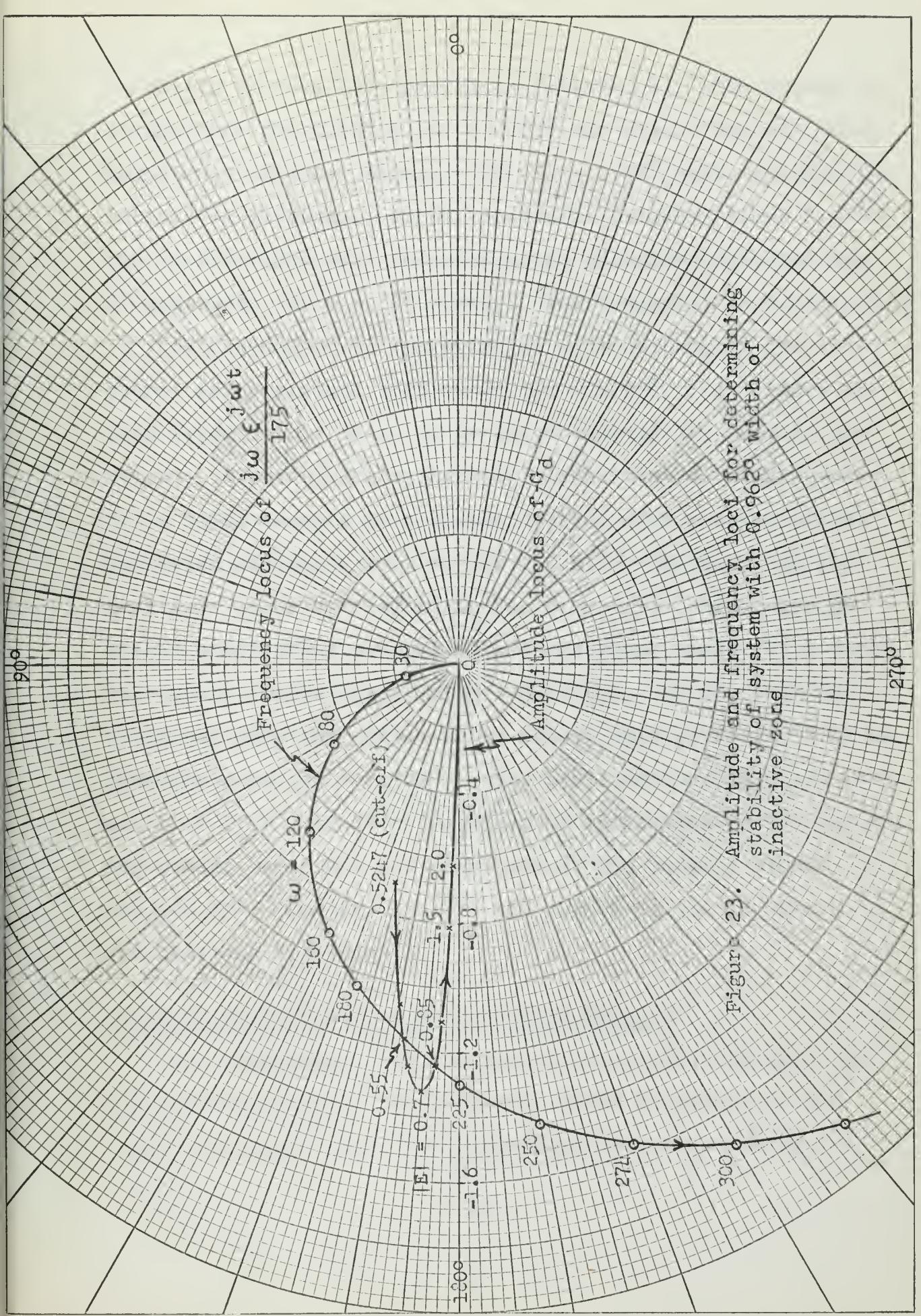
Figure 23. Amplitude and frequency loci for determining stability of system with 0.962° width of inactive zone

stability is then interpreted as follows [6]. The system is unstable for $0.57^\circ \leqslant |E| \leqslant 0.85^\circ$ and stable for all other magnitudes of error signal. If $|E| = 0.57^\circ$ sustained oscillations will result. If $|E|$ increases slightly above 0.57°, the oscillations will increase until sustained oscillations of magnitude $|E| = 0.85^\circ$ result. The frequency of oscillation is then determined by the point of intersection of the frequency and amplitude loci where $|E| = 0.85^\circ$. In Figure 23 this frequency is shown to be approximately 220 radians per second. A still larger increase in the control signal above $|E| = 0.85^\circ$ results in a stable system, with a decay of oscillation amplitude back to $|E| = 0.85^\circ$. The point on the amplitude locus corresponding to $|E| = 0.57^\circ$ represents unstable equilibrium conditions and the point where $|E| = 0.85^\circ$ represents stable equilibrium conditions. It may then be concluded that the system under study, when operating with an inactive zone, $\triangle = 0.962^\circ$, will oscillate continuously with an $|E| = 0.85^\circ$ and at a frequency of approximately 220 radians per second, provided the magnitude of the control signal, $|E| \geqslant 0.57^\circ$. For $|E| < 0.57^\circ$ the system is stable with no oscillations resulting.

Comparison of Predicted and Observed Results

For comparison with the predicted results outlined in the previous section the system as shown in Figure 11 was taken with zero input. This corresponds to the system

operating open-loop. The amplifier gain was then increased until an inactive zone, $\triangle = 0.962^{\circ}$ was obtained. The sustained oscillation which resulted had an amplitude of $\pm 1.51^{\circ}$ and a frequency of 225 radians per second. The predicted and observed frequencies of oscillation differ by approximately 2.3 percent. On the other hand, though the predicted and observed amplitudes are of the same order of magnitude, they differ considerably. Figure 23 shows the predicted amplitude to be 0.85°.

In many applications the discrepancy that was found to exist between predicted and observed amplitudes would be of little significance, however in some particular application closer correlation might be desirable. No attempt will be made in this study to fully justify this difference, however it is pointed out that the answer may be related to the shape of the waveform existing at the frequency of oscillation. Under the stated test conditions, the output waveform is also the input to the nonlinear device. At these higher frequencies, this waveform is triangular rather than sinusoidal as assumed for the application of describing function theory.

Degree of Stability

The absolute stability of the system has been discussed at some length in the previous sections. Of equal importance is the relative stability of the system. The system must possess sufficient damping so as to eliminate any undesirable

oscillation during the correction of a disturbance. For linear servomechanisms, Brown and Campbell [7] have established a rule of thumb procedure which gives an indication of the degree of stability from frequency response loci. A peak value M_p of the output-input ratio, θ_o/θ_i is determined. The rule states that in general there is adequate damping if $M_p < 1.3$. The rule is used widely in design work, however it naturally does not apply in all cases. Its use must be backed up by the designer's experience.

Kochenburger developed a similar rule for use in analyzing the relative stability of a contactor servomechanism [2]. Since the system under study functions similarly to a three-position contactor, Kochenburger's technique will be employed here in an effort to give the reader some feel for the relative stability of this system.

In this nonlinear system there is not just a single value of M_p over the frequency range. There is an M_p for each magnitude of control signal, E . These values of M_p and the associated frequencies, ω_p are determined graphically as follows. Referring to equation (17) it will

$$\frac{\theta_o}{\theta_i}(j\omega) \;=\; \frac{G_d}{G_s^{-1}\,\epsilon^{j\omega t} + G_d} \tag{17}$$

be noted that G_d is a fixed quantity for a given magnitude of the control signal, therefore to determine M_p , the peak

72

value of the ratio θ_0/θ_i , it is necessary only to determine

the denominator of equation (17) such that it is a minimum.

Taking as an example the system with a $\Delta = 2.01^\circ$, Figure 22 ,

which represents this system, is expanded and reproduced as

Figure 24 so that the graphical work will be more legible.

The quantity G_d of equation (17) is represented in Figure 24

by the vector $\overline{DO}$. The denominator of equation (17) is re-

presented by the vector sum $(\overline{DO} + \overline{OG})$ or the vector $\overline{DG}$. A

value of M is then determined graphically from the ratio of

vectors $\overline{DO}$ and $\overline{DG}$,

$$M = \frac{\overline{DO}}{\overline{DG}}$$

This, however, is the value of M corresponding to the fre-

quency $\omega = 50$ radians per second. M_p , being the peak

value of M over the frequency range, is determined by the

minimum value of $\overline{DG}$. The minimum length of $\overline{DG}$ is found

by drawing an arc of shortest possible radius from the point

D tangent to the frequency locus. $\overline{DG}_{min}$ is shown in Figure

24 for a magnitude of $|E| = 1.2^\circ$. Then merely by evaluating

the relationship

$$M_p = \frac{\overline{DO}}{\overline{DG}_{min}}$$

over the anticipated range of the error signal the loci, M_p

and ω_p versus $|E|$ may be obtained. These loci, for the

73
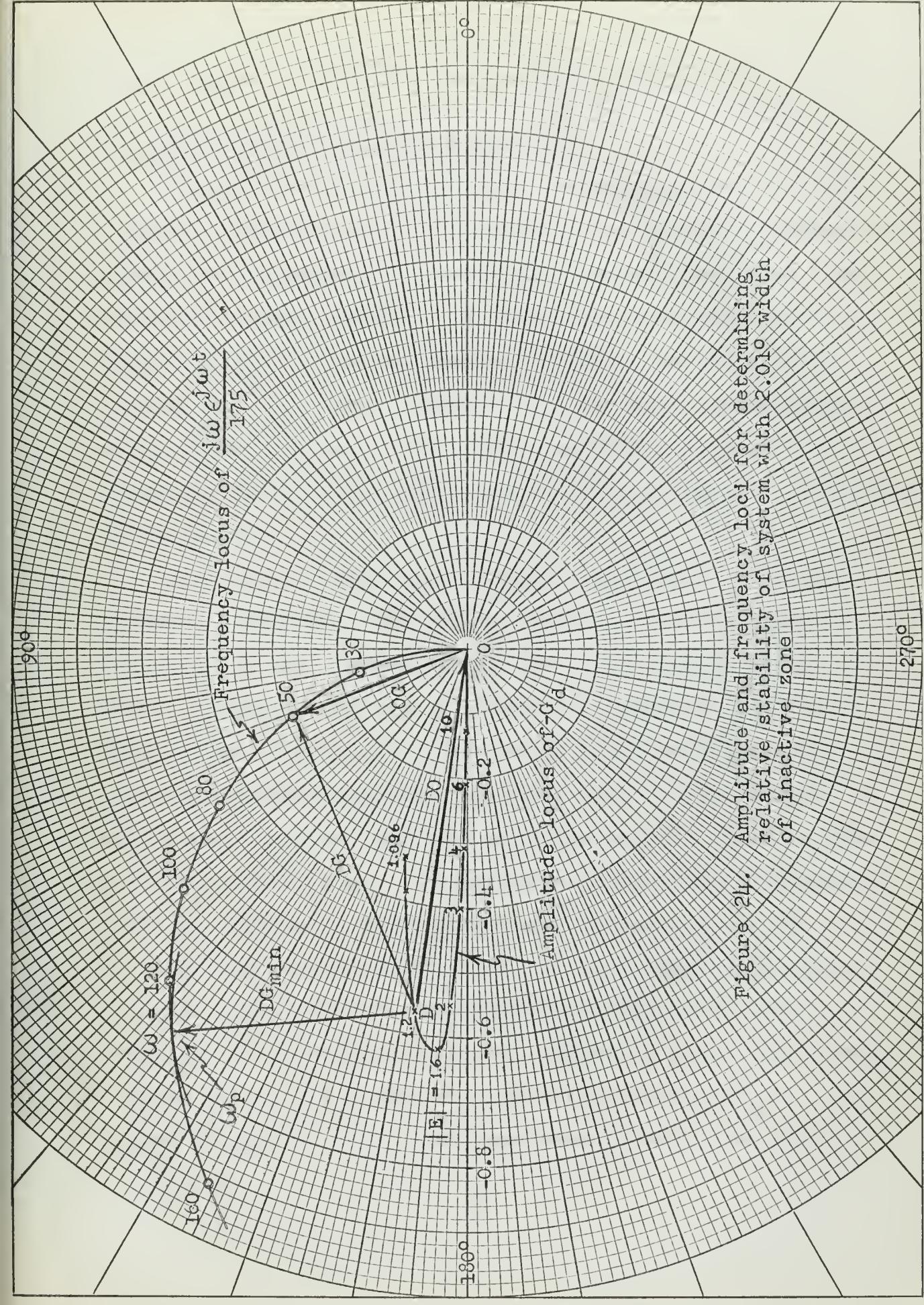
Figure 24. Amplitude and frequency loci for determining relative stability of system with 2.01° width of inactive zone

system where $\triangle = 2.01°$, are plotted in Figure 25.

Interpretation of Relative Stability

Figure 25 indicates that the system possesses excellent damping characteristics at relatively low natural frequencies during the beginning of a correction process involving high amplitude control signals. As the correction process nears completion the degree of damping decreases as revealed by a rise of the M_p locus, however M_p is never greater than 1.6 . At the lower values of $|E|$ the frequency associated with transient oscillations would increase considerably as indicated in Figure 25.

The authors, with their limited experience, will not attempt to interpret the full significance of the relative stability of this system within the scope of this study. It is not suggested that one evaluate the degree of stability of this system according to rules established by Kochenburger for contactor servomechanisms, nevertheless it is interesting to note these criteria, and then note the results shown in Figure 25 for this system. Kochenburger found from experimental tests on various types of contactor systems that an M_p of 2.0 near the cut-off point and of 1.3 for higher amplitudes of error signal provides a satisfactory degree of relative stability for most applications. Figure 25 shows this system to have an $M_p < 1.6$ near the cut-off point and $M_p \doteq 1$ at higher values of $|E|$. In other words, the system which

75
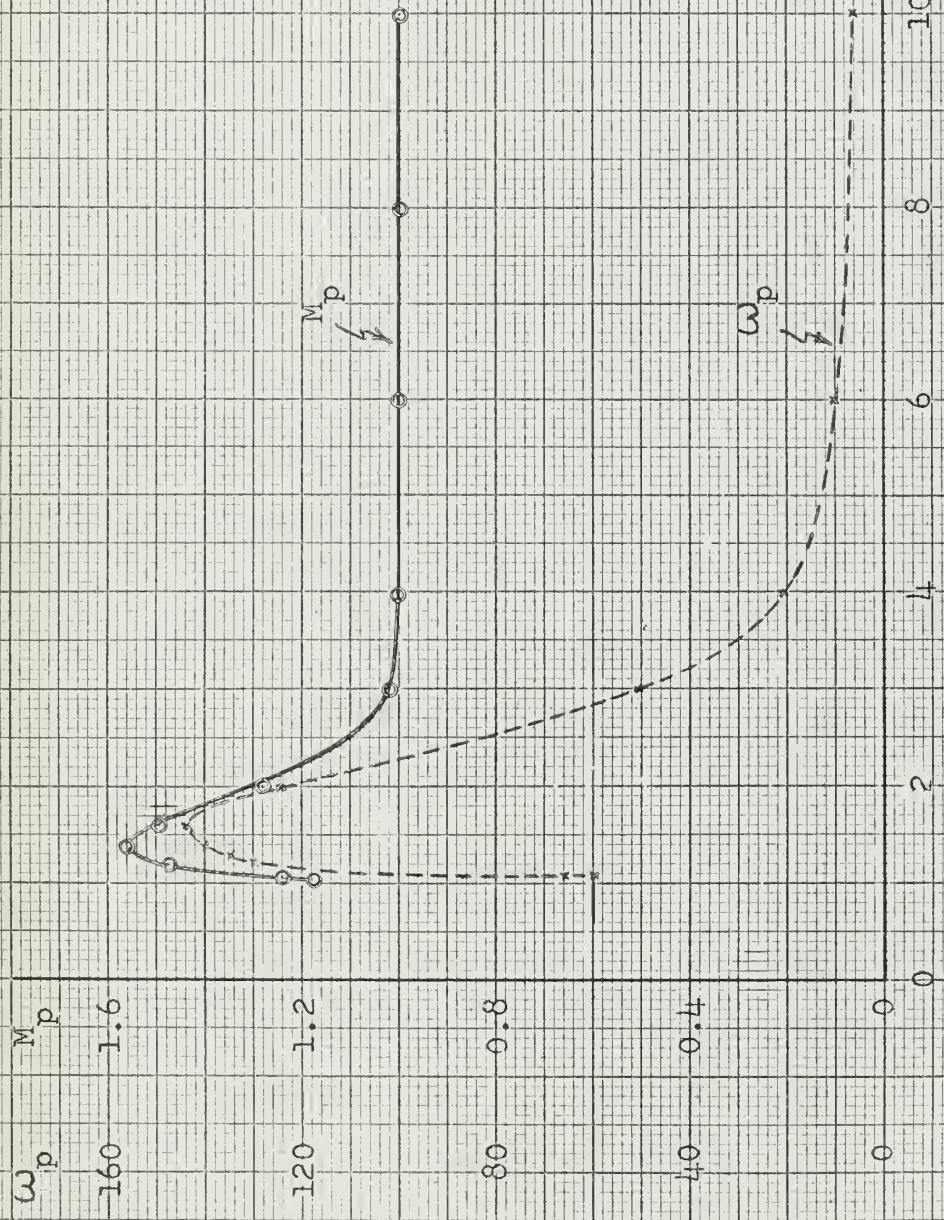
Figure 25. M_p and ω_p versus control signal amplitude, $|E|$.

is the subject of this study possesses a greater degree of
relative stability throughout the range of the control sig-
nal than is considered adequate for most contactor servo-
mechanisms.

CHAPTER VIII
CONCLUSIONS

This study demonstrates quite conclusively a mathemat-
ical technique for determining the closed-loop response char-
acteristics of a servo system employing the Curtiss-Wright
electromechanical spring clutch as the control device. It
has been shown that the closed-loop gain and phase loci
arrived at analytically by this technique agree very closely
with the actual results obtained from equipment tests. The
system bandwidth, which of course in a nonlinear system is a
function of the input signal amplitude, may be read directly
from the gain versus frequency locus.

While the calculations involved in arriving at the
closed-loop response of a system by the method employed in
this paper are quite straightforward, they are nevertheless,
extremely tedious. Therefore, where extensive use of this
technique is anticipated it is recommended that a digital
computer be used to perform the calculations.

The investigation into absolute system stability yielded
close agreement between theory and actual tests in the fre-
quency of the limit cycle oscillations. However, extremely
close agreement was not obtained between the theoretical and
actual amplitudes of these oscillations. The shape of the
control signal at these high frequencies is triangular and
it is the opinion of the authors that this may account for a

78

major part of the discrepancy in the amplitudes since the theory assumes a sinusoidal control signal.

Based on the relative stability criteria for contactor servomechanisms, a system employing the electromechanical spring clutch has adequate stability. Even though both systems function as on-off control systems, the validity of using such criteria is questionable, and it is believed that this is an area in which additional study might be done to definitely establish these stability criteria for a system employing the electromechanical spring clutch.

BIBLIOGRAPHY

1. Stuelpnagle and Dallas, Off-on Modulated Reversing
    Clutch Servo, Transactions AIEE, vol. 71, pt. II,
    pp. 406-410, 1953.

2. R. J. Kochenburger, Frequency Method for Analyzing
    and Synthesizing Contactor Servomechanisms, Trans-
    actions AIEE, vol. 69, pt. I, pp. 270-284, 1950.

3. E. Levinson, Some Saturation Phenomena in Servo-
    mechanisms with Emphasis on the Tachometer Stabi-
    lized System, Transactions AIEE, vol. 72, pt. II,
    pp. 1-9, 1953.

4. Davis and Ledgerwood, Clutches and Brakes, Control
    Engineers' Handbook, J. G. Truxal, Editor, sec. 14,
    McGraw-Hill Book Company, Inc., 1958.

5. R. J. Kochenburger, Principles of On-off Control,
    Control Engineers' Handbook, J. G. Truxal, Editor,
    sec. 10, McGraw-Hill Book Company, Inc., 1958.

6. J. G. Truxal, Control System Synthesis, chap. 10,
    McGraw-Hill Book Company, Inc., 1955.

7. Brown and Campbell, Principles of Servomechanisms,
    John Wiley and Sons, 1948.